Effect of the structural modification of Candesartan with Zinc on hypertension and left ventricular hypertrophy

Valeria R. Martinez, Augusto Martins Lima, Nikolaous Stergiopulos, Jorge O. Velez Rueda, Maria S. Islas, Mercedes Griera, Laura Calleros, Manuel Rodriguez Puyol, Carolina Jaquenod de Giusti, Enrique L. Portiansky, Evelina G. Ferrer, Verónica De Giusti, Patricia A.M. Williams

PII: S0014-2999(23)00165-6

DOI: https://doi.org/10.1016/j.ejphar.2023.175654

Reference: EJP 175654

To appear in: *European Journal of Pharmacology*

Received Date: 31 October 2022

Revised Date: 25 February 2023

Accepted Date: 9 March 2023

Please cite this article as: Martinez, V.R., Martins Lima, A., Stergiopulos, N., Velez Rueda, J.O., Islas, M.S., Griera, M., Calleros, L., Rodriguez Puyol, M., Jaquenod de Giusti, C., Portiansky, E.L., Ferrer, E.G., De Giusti, Veró., Williams, P.A.M., Effect of the structural modification of Candesartan with Zinc on hypertension and left ventricular hypertrophy, *European Journal of Pharmacology* (2023), doi: https://doi.org/10.1016/j.ejphar.2023.175654.

Author statement

- Conceptualization: VRM, AML, VDG, PAMW
- Formal analysis: VRM, MSI, CJDG
- Funding acquisition: NS, MRP, ELP, VDG, PAMW
- Investigation: VRM, MSI, MG, JOVR, ELP, CJDG
- Methodology: VRM, AML, LC, CJDG
- Project administration: NS, MRP, ELP, VDG, PAMW
- Resources: AML, JOVR, MG, LC, PAMW
- Supervision: AML, VDG, EGF, PAMW
- Validation: AML, VDG, MRP, PAMW
- Visualization: VRM
- Writing – original draft: VRM, MSI, CJDG
- Writing – review & editing: AML, VDG, ELP, MRP, EGF, PAMW

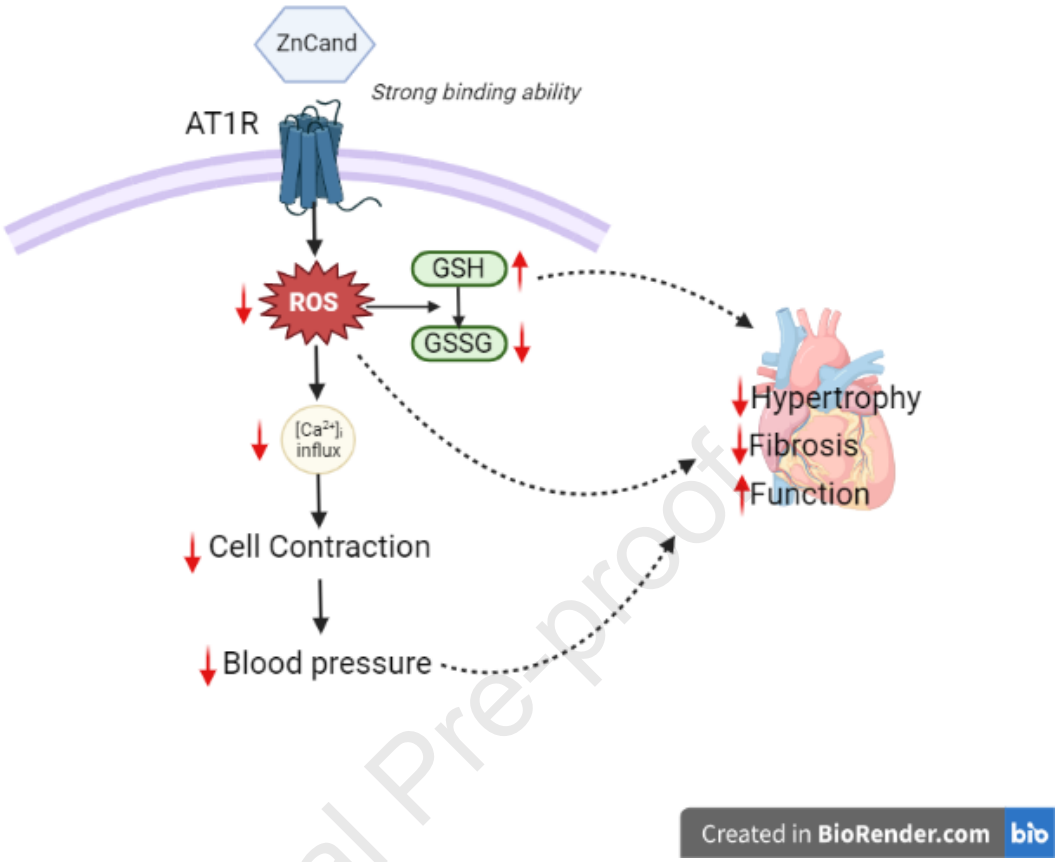

Effect of the structural modification of Candesartan with Zinc on hypertension and left ventricular hypertrophy

Valeria R. Martinez[1,2], Augusto Martins Lima[3], Nikolaous Stergiopulos[3], Jorge O. Velez Rueda[2], Maria S. Islas[4], Mercedes Griera[5], Laura Calleros[5], Manuel Rodriguez Puyol[5], Carolina Jaquenod de Giusti[2], Enrique L. Portiansky[6], Evelina G. Ferrer[1], Verónica De Giusti[2,*], Patricia A.M Williams[1,*]

[1] CEQUINOR-CONICET-CICPBA-UNLP, Facultad de Ciencias Exactas, Universidad Nacional de La Plata, Bv. 120 N◦ 1465, 1900 La Plata, Argentina

[2] CIC-CONICET-UNLP, Facultad de Médicas, Universidad Nacional de La Plata, 60 y 120, 1900 La Plata, Argentina

[3] Laboratory of Hemodynamics & Cardiovascular Technology (LHTC), Institute of Bioengineering (Bâtiment MED), Station 9, École Polytechnique Fédérale de Lausanne, 1015 Lausanne, Switzerland

[4] Departamento de Química y Bioquímica, Facultad de Ciencias Exactas y Naturales, Universidad Nacional de Mar del Plata, 7600, Mar del Plata, Argentina

[5] Departamento de Fisiología, Universidad de Alcalá, Campus Universitario, 28871-Alcalá de Henares, Madrid, Spain

[6] Laboratorio de Análisis de Imágenes-UNLP, Facultad de Ciencias Veterinarias, Universidad Nacional de La Plata, 60 y 118, 1900 La Plata, Argentina

*Corresponding authors.

e-mail address: vdegiusti@med.unlp.edu.ar (V. De Giusti); williams@quimica.unlp.edu.ar (P.A.M. Williams)

Abstract

Hypertension is the most common cause of left ventricular hypertrophy, contributing to heart failure progression. Candesartan (Cand) is an angiotensin receptor antagonist widely used for hypertension treatment. Structural modifications were previously performed by our group using Zinc (ZnCand) as a strategy for improving its pharmacological properties. The measurements showed that ZnCand exerts a stronger interaction with the angiotensin II receptor, type 1 (AT_1 receptor), reducing oxidative stress and intracellular calcium flux, a mechanism implied in cell contraction. These results were accompanied by the reduction of the contractile capacity of mesangial cells. *In vivo* experiments showed that the complex causes a significant decrease in systolic blood pressure after 8 weeks of treatment in spontaneously hypertensive rats (SHR). The reduction of heart hypertrophy was evidenced by echocardiography, the histologic cross-sectional area of cardiomyocytes, collagen content, the B-type natriuretic peptide (BNP) marker and connective tissue growth factor (CTGF) and the matrix metalloproteinase 2 (MMP-2) expression. Besides, the complex restored the redox status. In this study, we demonstrated that the complexation with Zn(II) improves the antihypertensive and cardiac effects of the parental drug.

Keywords

Hypertension; Zn-Candesartan; cardiac hypertrophy; oxidative stress

Statements and Declarations

There are no conflicts to declare

Graphical abstract

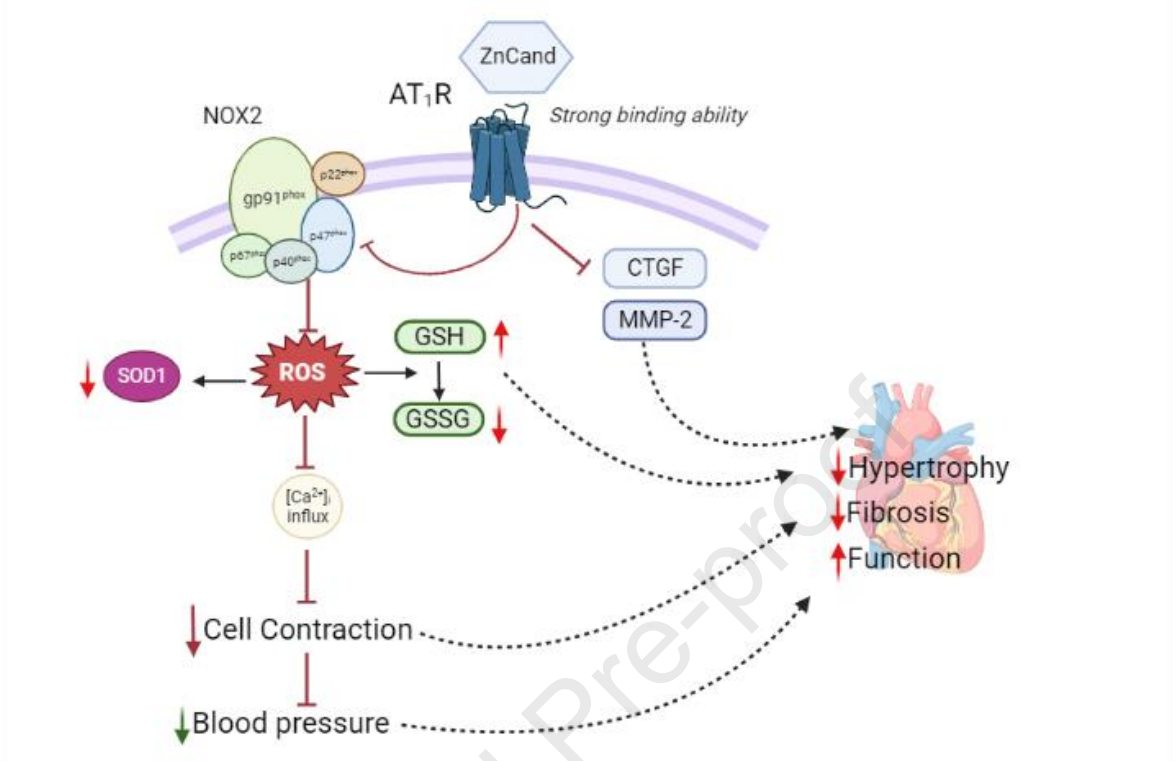

1. Introduction

Hypertension is the most important risk factor involved in the development of left ventricular hypertrophy (LVH) as a response to chronic pressure overload (Aronow, 2017). The abnormalities of the ventricle, generated by fibrosis and geometrical changes, contribute to the progression of heart failure (Gradman and Alfayoumi, 2006). The sustained hypertrophic stimulation and the increase of oxidative stress, which cannot be adequately countered by intrinsic antioxidant systems, worse the cardiac function (Takimoto and Kass, 2007). It has been demonstrated that blood pressure lowering treatment with angiotensin II receptor blockers (ARB) reduces LVH and improves cardiac function (Brown et al., 2001). The ARB Candesartan (Cand), independently of its blood pressure lowering effect, attenuates reactive

oxidative species (ROS) production. However, its low affinity to the angiotensin II receptor in comparison to other ARB leads to a slight improvement in heart function (Sakamoto et al., 2015).

Bioinorganic compounds in medicine offer possibilities for designing therapeutic agents with increased efficiency, bioavailability, and low toxicity (Bruijnincx and Sadler, 2008; Mjos and Orvig, 2014). Considering that Zinc is the second most important transition metal in the body, and, because it is a d^{10} transition metal, it exclusively forms a Zn^{2+} ion and typically assembles coordination complexes in a tetrahedral geometry, maintaining the structure and stability of molecules with Nitrogen, Oxygen and Sulfur groups (Pace and Weerapana, 2014). Considering these facts, our strategy to enhance the pharmaceutical properties, consisted of the introduction of a structural modification of candesartan (Cand) with Zn(II) coordination (ZnCand), Fig. 1, to obtain a new compound with more beneficial effects on the hypertensive cardiovascular injury. We have previously reported the synthesis, the physicochemical characterization and the antitumoral activity of the ZnCand complex ($[ZnCand(H_2O)_2].2H_2O$) (Martínez et al., 2021a). Additionally, we evaluated the biodistribution capacity through the serum albumin interaction (Martínez et al., 2022). Besides, we have demonstrated that the complexation of an ARB (Telmisartan) with Zinc (ZnTelm) ameliorates its antihypertensive properties (Martínez et al., 2021b). In the present work, we examined *in vitro* the interaction of ZnCand to the angiotensin II receptor, type 1 (AT_1 receptor), the ROS production and the contractile response of the human mesangial cell line, HMC. Moreover, we performed *in vivo* studies in spontaneous hypertensive rats (SHR), elucidating its

antihypertensive and antihypertrophic effects. We also compared the effects of ZnCand against free Cand, to demonstrate that the structural changes induced on the antihypertensive drug upon metal coordination are responsible for the improvement of the biological effects proposed for ZnCand.

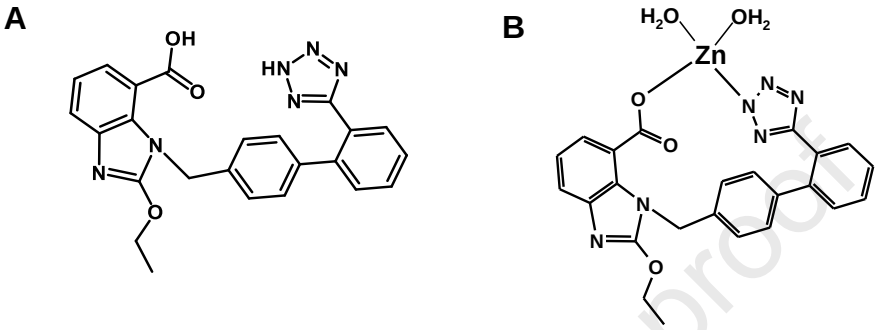

Fig. 1. Chemical structures of (A) candesartan 2-(ethyloxy)-1-{[2'-(1H-tetrazol-5-yl)biphenyl-4-yl]methyl}-1H-benzimidazole-7-carboxylic acid and (B) ZnCandesartan ([ZnCand(H_2O)$_2$].2H_2O)

2. Materials and Methods

2.1. Reagents

Candesartan was purchased from Rhundu Pharma, China, and Zinc(II) chloride was purchased from Biopack, Argentina. A pCXN2-HA-AT1R-YFP plasmid containing the human angiotensin II receptor, type 1 (AT_1 receptor) and the yellow fluorescent protein (YFP) was purchased from Addgene (Addgene plasmid # 101659).

2.2. In vitro procedures

2.2.1. Cell Culture

Human embryonic kidney 293 cells (HEK293) were maintained at 37ºC in 5% CO_2 and Dulbecco's modified Eagle's medium (DMEM, Gibco) supplemented with 10%

fetal bovine serum (FBS) without antibiotics. For transient transfections, ~1 × 10^6 cells/mL were cultured on 8-well chamber glass slides or in 48-well plates coated with poly-D-lysine. After 24 h at 60-70 % confluence, transfections were performed using Lipofectamine 3000 reagent (Invitrogen) in OPTI-MEM medium (Gibco) with the pCXN2-HA-AT1R-YFP plasmid according to the manufacturer's instructions (Inuzuka et al., 2016). After 48 h post-transfection, the assays were carried out.

Human mesangial cells (HMC) were maintained in the same condition cultured with Roswell Park Memorial Institute medium (RPMI 1640, Gibco), 10% FBS and penicillin-streptomycin antibiotics. A density of approximately 2 × 10^5 cells/mL was plated on 35-mm plates and studies were performed before they reached confluence.

2.2.2. Interaction with the angiotensin type I receptor AT_1 receptor

2.2.2.1. Competitive binding assay, ROS, Ca^{2+} flux

The competitive binding assays were performed using a previously described procedure (Bragina et al., 2017). Briefly, 10 μM of Ang II labeled with tetramethylrhodamine (TAMRA-Ang II) (AnaSpec, Inc. Fremont, CA) was used for the binding assays in presence of 0.1 μM, 1 μM, or 10 μM of Cand, ZnCand, or 10 μM unlabeled Angiotensin II (for nonspecific binding). All the compounds were dissolved in 0.5% DMSO in Hank's balanced salt solution (HBBS, Gibco) and were incubated with the cells for 90 min placed on ice. After incubation, the slides were washed with ice- cold Phosphate-buffered saline solution (PBS) and mounted with Vectashield Mounting Medium with DAPI (4′,6-diamidino-2-phenylindole) to stain nuclei. All specimens were examined using a confocal laser microscope (Zeiss

LSM700). The signal intensity was measured (mean grey value) and normalized by counting the DAPI-stained nuclei. The difference between total binding and nonspecific binding is defined as the specific binding. The concentration of TAMRA-Ang II and unlabeled Ang II were selected according to previous reports (Grießner et al., 2009; Martínez et al., 2021b). No cytotoxic effects were found in human embryonic kidney HEK293 treated cells (Fig. S1)

Dihydroethidium (DHE) was used to assess cellular ROS production by Ang II, working with a modified method proposed by Choi et al. (Choi et al., 2008). Briefly, transfected cells were plated into poly-D-lysine-coated, black-walled 96-well plates. They were incubated with 10 µM of Ang II alone or 10 µM Ang II plus the compounds at the selected concentrations for 24 h. The concentration of Ang II was chosen for comparison with binding experiments. Next, incubation with 10 µM DHE for 1 h at 37 °C under light protection was performed and the fluorescence intensity (λ_{exc} = 536 nm and λ_{em} = 635 nm) was measured using a microplate reader (Tecan infinite 500). The Ca^{2+} flux was determined using the non-invasive radiometric calcium indicator Fura-2 AM (Fura-2 acetoxymethyl ester) that crosses cell membranes and the acetoxymethyl group was removed by cellular esterases. For bonded Ca^{2+}-Fura-2, λ_{exc} = 340 nm and for free Ca^{2+}- Fura-2, λ_{exc} = 380 nm, being λ_{em} = 510 nm, for both states. Transfected HEK 293 cells were seeded onto poly-D-lysine-coated, black-walled 96-well plates. Cells were washed with 1-2 mL of HEPES-buffered saline (HBS) (145 mM NaCl, 5 mM KCl, 10 mM HEPES, 1 mM $MgCl_2$, and 10 mM glucose) and incubated for 1h in the dark with 5 µM Fura-2 AM with 0.05% Pluronic F-127, at room temperature. The dye was aspirated and, after the addition of 100 µl of HBS,

intracellular Ca^{2+} levels were subsequently measured. After the first reading, 100 µL Ang II 10 µM dissolved in HBS buffer was added. The remaining wells were pretreated with 100µL of the compounds at the selected concentrations. Then, 100 µL of 10 µM Ang II was added. The fluorescence intensity was captured at 28 °C for 90 sec with kinetic intervals of 9 sec after compound addition in a fluorometric plate reader. For standard curves, 1 mM of $CaCl_2$ (high calcium) and 10 mM EDTA (zero calcium) was used. The standard radiometric dye formula developed by Grynkiewicz (Grynkiewicz et al., 1985), $[Ca^{2+}] = K_d\beta[(R-R_{min})/(R_{max}-R)]$ was used to determine calcium concentrations, where, K_d represents the dissociation constant of Fura-2 (224 nM), R_{min} is the ratio for zero calcium, R_{max}, the ratio for high calcium, β is the ratio of fluorescence of zero calcium to the fluorescence of high calcium (380 nm), and R is the experimental ratio of the fluorescence at 340 nm to the fluorescence at 380 nm.

2.2.2.2. Determination of changes in planar cell surface area (PCSA)

Human mesangial cells (HMC) cells were pretreated with either 0.01 or 1 µM of the different compounds (Cand, ZnCand or $ZnCl_2$). After 15 min, 1 µM Ang II was added, as was described in previous reports (Islas et al., 2016). Photographs of cells were captured at 0 min and after 30 min of Ang II addition. Every cell with a sharp margin suitable for the planimetric analysis was considered. Eight cells *per* image were analysed. PCSA was determined by using ImageJ2 software (NIH). The negative control was performed without adding Ang II, while it was added in the positive control.

2.2. In vivo procedures

2.2.1. Animals

All the procedures were performed in accordance with the Guide for the Care and Use of Laboratory Animals (NIH Publication No. 85-23, revised 1996) and the experimental protocol was approved by the Institutional Animal Ethics Committee of La Plata University School of Medicine (P02-03-2021). Three-month-old male spontaneously hypertensive rats (SHR) (n=26; body weight 300-400 g) were randomly divided in four groups: a) control group treated with tap water (Control-SHR), b) group treated with candesartan (10 mg/kg/day; Cand-SHR), c) group treated with ZnCand (13 mg/kg/day; ZnCand-SHR), d) group treated with $ZnCl_2$ (2.8 mg/kg/day; Zn-SHR). The compounds were administrated for 8 weeks in the drinking water, controlling the drink volume. Every 3 days the solutions were replaced. The doses of candesartan were selected based on earlier reports. ZnCand and $ZnCl_2$ were administered in molar equivalent doses of candesartan. Body weight was controlled weekly. It was determined that the compounds had no significant effect on the animals' body weight or water intake. Besides, neither dead animals nor adverse effects were observed during the administration of ZnCand.

2.2.2. Blood pressure and echocardiographic evaluation

Systolic blood pressure (BP) was measured by the tail-cuff plethysmography once a week. Rats were monitored echocardiographically at the beginning and the end of the experimental period. Rats were lightly anesthetized with 1-2% isofluorane under oxygen flow to perform 2-dimensional M-mode echocardiography with a 15-MHz transducer (Terason 3000). Measurements were made using criteria analogous to

those recommended by the American Society of Echocardiography(Jones et al., 1992). Left ventricular mass (LVM) was calculated according to Devereaux and Reichek(Devereux and Reichek, 1977), and the LVM index (LVMI) was calculated as the quotient between the LVM and the body weight. Fractional shortening was calculated as ([(LVDd-LVDs)*100]/LVDd) (LVDd: diastolic left ventricular diameter; LVDs: systolic left ventricular diameter).

2.2.3 Ventricular Myocyte Isolation

Rat ventricular myocytes were isolated according to the technique previously described (Louch et al., 2011). Briefly, the hearts were attached via the aorta to a cannula, rapidly excised, and mounted in a Langendorff perfusion apparatus. They were then retrograde perfused at 37 °C with HEPES–based salt “isolation” solution with the following composition: 146.2 mM NaCl, 4.7 nM KCl, 1 mM $CaCl_2$, 10 mM HEPES, 0.35 mM NaH_2PO_4, 1 mM $MgSO_4$, and 10 mM glucose (pH adjusted to 7.4 with NaOH 1N). The solution was continuously bubbled with 100% O_2. When the coronary circulation was cleared of blood, perfusion was continued for 5 min with Ca^{2+}-free isolation solution containing 0.1 mM EGTA, and then for 15 min with a solution containing 0.05 mM $CaCl_2$, 0.5 mg/mL collagenase type II (300 U/mL), 0.025 mg/mL protease, and 1.25 mg/mL BSA at 37 °C. After digestion, the heart was cut down, and the ventricular tissue was mechanically dissociated. The desegregated myocytes were separated from the undigested tissue and rinsed several times with the isolation solution containing 1% BSA. The $CaCl_2$ concentration of the solution was increased in 4 steps to 1 mmol/L. Myocytes were maintained in 1 mmol/L $CaCl_2$

in isolation solution at room temperature (20°C to 22°C) until their use in the experiments.

2.2.4 Measurements in Isolated Myocytes

2.2.4.1 Calcium transient measurement

Cardiomyocytes were loaded with Fura-2 AM (final concentration: 3 µM) during 12 min. The cells were placed in a perfusion chamber on an inverted microscope (Nikon TE2000-U) adapted for epifluorescence by an IonOptix hardware. The cardiomyocytes were stimulated via two platinum electrodes at 0.5 Hz. Simultaneously, the ratio of the Fura-2 fluorescence (510 nm) obtained after exciting the dye at 340 and 380 nm was taken as an index of Ca^{2+}_i.

2.2.4.2 ROS determination

Isolated cardiomyocytes were incubated with the H2DCFDA probe (2,7-dichlorodihydrofluorescein diacetate) at a final concentration of 10 µM for 30 min at 37 °C under light protection. Subsequently, cells were lysed with 0.1% Triton X-100. Intracellular ROS were detected on the Thermofisher Varioskan spectrofluorometric multiplate reader using excitation wavelength at 485 nm and emission at 520 nm. The protein content was estimated using the Bradford technique(Bradford, 1976)

2.3. Ex vivo procedure

2.3.1. Morphometric parameters

At the end of the experiment, SHR rats were weighed (body weight, BW), euthanized with urethane (1g/kg) via intraperitoneal, and the hearts were dissected and

weighed. Then, the atrial tissues, ventricles, and large vessels were carefully cut. The right ventricle was left out and only the left ventricular mass (LVM) was determined. The tibial lengths (TL) were measured. The LVM/TL ratio and left ventricular mass index, as the ratio LVM/BW were calculated to evaluate the hypertrophic response.

2.3.2. Cross-sectional area measurement

Ventricular tissue was fixed in buffered 10% formaldehyde and paraffin-embedded. LV sections (5 μm thick) at the equators were stained with hematoxylin-eosin for determining cardiomyocyte cross-sectional area (CSA). To assess CSA, only round to ovoid cells with visible round nuclei were considered and 50 cells were counted in at least 10 images obtained from each left ventricle. All the stained sections were observed under the microscope (Olympus BX53, Japan) and the images were captured using a digital video camera (Olympus DP71, Japan). Images were analyzed using computer software (Image-Pro Plus, v.6.3, Media Cybernetics, MD). The investigator responsible for the morphological analysis was blinded to each experimental group.

2.3.3. Collagen determination

Five 5 μm thick coronal sections of the left ventricle were stained using the Picrosirius red technique (Direct Red 80, Aldrich, Milwaukee, WI 53233, USA) for collagen evaluation. Samples were observed under polarized light. An analyzer (U-ANT, Olympus) and a polarizer (U-POT, Olympus) were used to study the birefringence of the stained collagen. Histological (20× magnification) images were

digitized using a digital video camera (Olympus DP71, Japan) mounted on a widefield microscope (Olympus BX53, Japan). Captured images were saved in TIF format using image analysis software ((Image-Pro Plus, v.6.3, Media Cybernetics, MD).

2.3.4. Real-time qPCR for BNP determination

RNA was extracted from left ventricle homogenates using TRIzol reagent (Life Technologies, Carlsbad, CA). cDNA was generated by reverse transcriptase reaction using M-MLV RT (Promega, Madison, Wis). Real-time quantitative polymerase chain (qPCR) was performed on cDNA using the IQ SYBR green Super Mix (Bio-Rad, Hercules, Calif) and iCycler iQ (Bio-Rad, Hercules, Calif). The following primers were used:

BNP Gene Sense: CCCAGATGATTCTGCTCCTG, Antisense: TTCTGCATCGTGGATTGTTC.

The relative abundance of RNA was calculated by the ΔΔCt method (CT, threshold cycles), with ΔCT = CT(target gene)−CT(reference gene) and ΔΔCT = ΔCT(target sample)−ΔCT(reference sample). Primers were designed using Primer-Blast (NCBI, NIH). Primers were designed using Primer-Blast (NCBI, NIH). All primers were 90% to 110% efficient, as assessed by the standard curve, and all displayed only one dissociation peak.

2.3.5. ROS determination

100 mg of rat left ventricular tissue was homogenized on ice using 2 mL of ice-cold Tris-HCl buffer (40 mM, pH = 7.4) (Pro Scientific Bio-gen PRO200 Hand-Held

homogenizer). Tissue homogenates (100 µL) were incubated for 40 min at 37 °C with 2 mL of a solution of H_2DCFDA diluted 1:200 in Tris-HCl buffer (final concentration: 10 µM). As control of tissue autofluorescence, 100 µL of tissue homogenate was incubated with 2 mL of Tris-HCl buffer under the same conditions(Mousavi et al., 2020). The fluorescence intensity of the samples was assessed using a RF-Shimadzu 6000 spectrofluorometer (λ_{ex} = 485 nm and λ_{em} = 525 nm).

2.3.6. GSH and GSSG measurement

The reduced (GSH) and oxidized (GSSG) glutathione levels in the heart tissue were assessed by the Hissin and Hilf modified fluorometric method(Hissin and Hilf, 1976). 100 µL of tissue homogenates were mixed with 1.8 mL of ice-cold phosphate buffer (Na_2HPO_4 0.1M-EDTA 0.005 M, pH 8) and 100 µL of 0.1% methanolic solution of o -phthaldialdehyde (OPT) were added. For GSSG measurements and to mask GSH contents, 100 µL of homogenates were incubated with 0.04 M of N-ethylmaleimide (NEM), then ice-cold NaOH (1.8 mL, 0.1 M, pH 12) was added to hydrolyze GSSG, with a final addition of 0.1% of OPT. Fluorescence measurements were performed at 420 nm (λ_{exc} = 350 nm). Calibration curves using GSH and GSSG as standard solutions (Sigma-Aldrich) were used to calculate the amount of GSH and GSSG. The ratio was expressed as a percentage of the control.

2.3.7. Western Blot Analysis

Left ventricle samples were stored in aliquots at −80 °C for further use. Next, samples were homogenized in a RIPA (Radio-Immunoprecipitation Assay) lysis

buffer (200 mg/mL) supplemented with protease and phosphatase inhibitors cocktail. After centrifugation, the protein content in the supernatant was determined through Bradford method (Bradford, 1976). Protein samples (were separated by electrophoresis on a 10% sodium dodecyl sulfate-polyacrylamide gel (SDS-PAGE) and transferred to PVDF (Polyvinylidene Difluoride) membranes. Next, membranes were blocked with non-fat-dry milk and incubated overnight with anti-CTGF (sc-365970; Santa Cruz Biotechnology, 1:1000), anti-MMP2 (sc-13595; Santa Cruz Biotechnology, 1:1000), anti-SOD 1 (sc-17767; Santa Cruz Biotechnology, 1:1.000), anti-SOD 2 (sc-137254 ; Santa Cruz Biotechnology, 1:1.000), anti-p91 (sc-130548 ; Santa Cruz Biotechnology, 1:1.000),. As internal control, anti-GAPDH, glyceraldehyde 3-phosphate dehydrogenase, (sc-47724, Santa Cruz Biotechnology, 1:1.000), anti-Na^+/K^+ (ST0533, Thermofisher, 1:1.000) were used. Peroxidase conjugated anti-rabbit (sc-2004; Santa Cruz Biotechnology, 1:10.000) or anti-mouse Ig-G H&L (ab 205719; Abcam, 1:10.000) were used as secondary antibodies and bands were visualized using the Immobilon Western Chemiluminescent HRP Substrate (Merck). Blots were visualized using a Chemidoc Image Station (Bio-Rad) and quantified by densitometric analysis (Image J Fiji).

2.4. Statistics

GraphPad Prism 9 (GraphPad, San Diego, CA) was used for the plots and statistical analysis. Data were expressed as means ± SEM and were compared with Student's t-test or one-way ANOVA followed by the Tukey post hoc test. A value of $p < 0.05$ was considered statistically significant.

3. Results

3.1. ZnCand had a stronger interaction with the AT_1 receptor than candesartan, decreased ROS production, reduced Calcium flux and the contraction of the planar cell surface area (PCSA) induced by AngII

To study the interaction of ZnCand with the AT_1 receptor and to compare to Cand alone, transient transfected HEK 293 cells were incubated with three different concentrations of Cand and ZnCand (0.1, 1 and 10 µM) and 10 µM TAMRA-Ang II (

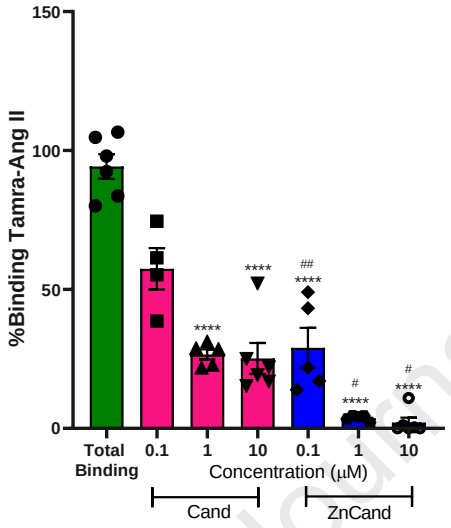

Fig. 2). The TAMRA-Ang II binding decreases as the compound concentration increases. For all concentrations, the complex showed a better blocking effect on the AT_1 receptor, demonstrating that the more rigid structure of candesartan produced by metal complexation can bind strongly to the receptor. These findings suggest that a lower concentration of ZnCand (0.1 µM) is enough to induce a similar blocking effect on the AT_1 receptor than that produced by higher concentrations of Cand (1 and 10 µM). Results of TAMRA-Ang II and TAMRA-Ang II + Ang II salt incubations are shown in the supplementary section (Fig. S3). Non-transfected cells

were tested with TAMRA-Ang II as a negative control, and 0.5% DMSO and TAMRA-Ang II were evaluated on transfected cells to exclude the vehicle effect (data not shown).

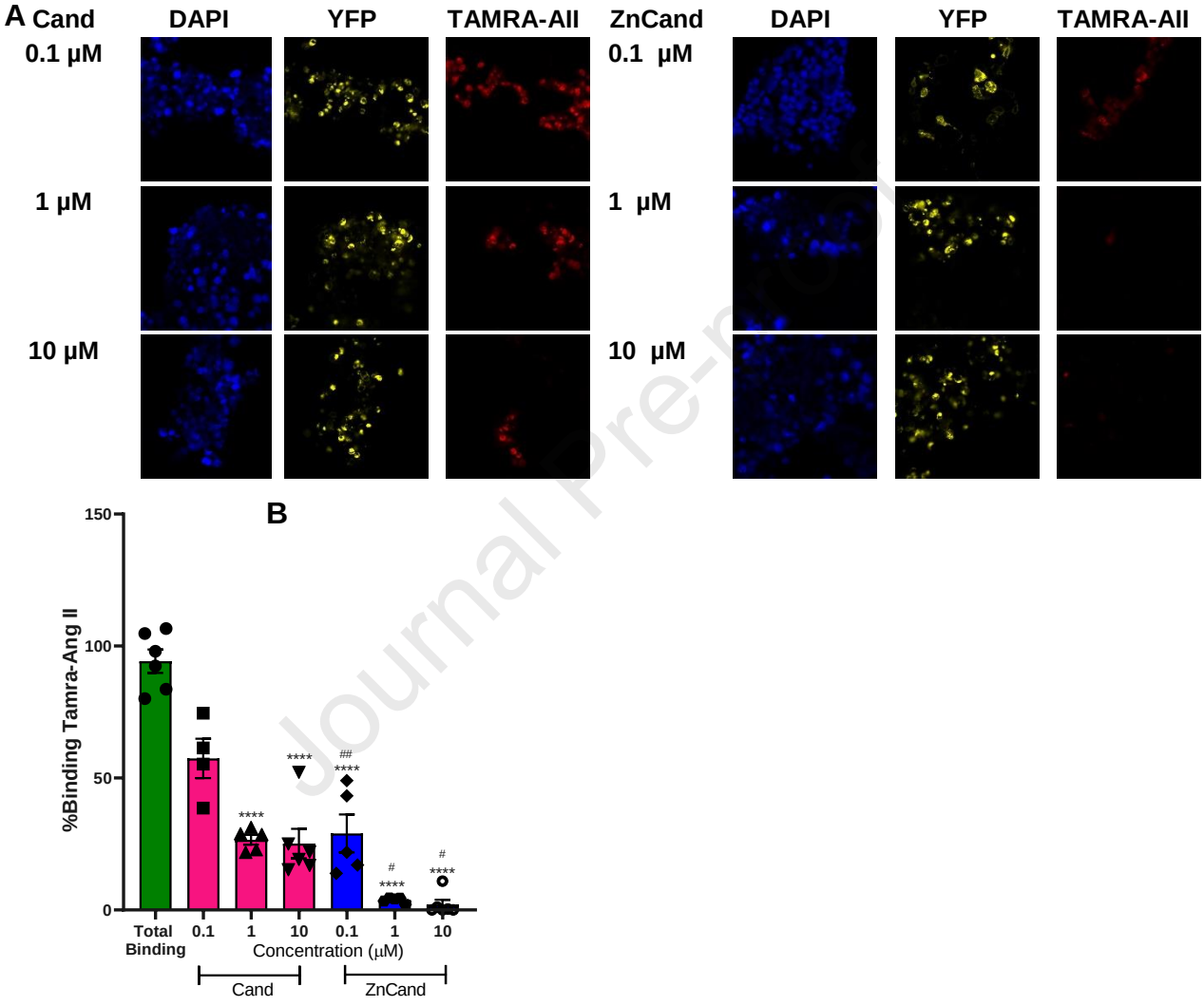

Fig. 2. A: representative confocal images of transient transfected HEK293 cells expressing YFP-tagged AT_1 receptor (yellow) and nuclei stained with DAPI (blue) incubated with Cand and ZnCand (0.1, 1 or 10 µM) and 10 µM TAMRA-Ang II (red). TAMRA-Ang II bound to AT_1 receptor was considered as total binding (100%) and TAMRA-Ang II plus 10 µM Ang II defined the nonspecific binding (0%). B: Bar plot

representing the percentage of TAMRA-AngII binding. Data are expressed as mean ± SEM. (*) Values statistically significant between Cand or ZnCand and control (****p<0.0001), ($^{\#}$) Values statistically significant between Cand and ZnCand at the same concentration ($^{\#}$p<0.05; $^{\#\#}$p<0.01)

It is known that Ang II stimulates ROS generation in vascular and cardiac cells (Virdis et al., 2011) and the antagonism of its receptor can reverse these levels (Montezano et al., 2014). Based on the above results, we examined if a stronger AT_1 receptor blockade leads to a better Ang-induced ROS production inhibition. Transfected HEK 293 cells were incubated with Ang II alone and Ang II plus the three concentrations of Cand or ZnCand (0.1, 1 and 10 µM). As expected, Ang II significantly increased ROS production, which was prevented with Cand and ZnCand treatment in a concentration-dependent manner. Interestingly, 10 µM ZnCand reduced ROS production, reaching values similar to control (cells without Ang II treatment). Besides, ZnCand at low concentrations exerted similar effects to those of Cand at high concentrations (Fig. 3).

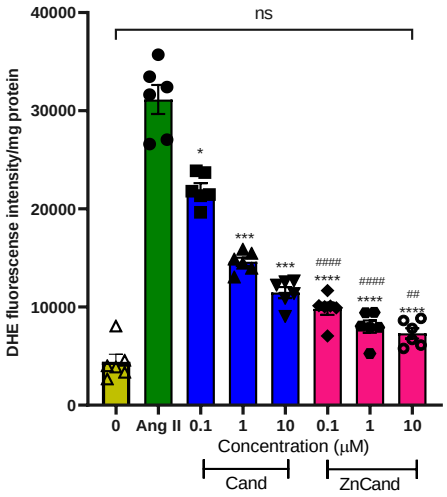

Fig. 3. Bars graph representing ROS production in transfected HEK293 cells after being treated with Ang II alone and Ang II plus three different concentrations of Cand or ZnCand (0.1, 1 and 10 μM). Data are expressed as mean ± SEM. (*) Values statistically significant between Cand or ZnCand and control (***p<0.001; ****p<0.0001), ($^{\#}$) Values statistically significant between Cand and ZnCand at the same concentration ($^{\#\#}$p<0.01; $^{\#\#\#\#}$p<0.0001)

Since Ang II signaling causes an increase in vascular ROS by stimulating the nicotinamide adenine dinucleotide phosphate (NADPH) oxidases and directly elevates cytosolic Ca^{2+}, the major determinant of contraction (Touyz, 2005), we investigated the relationship between the AT_1 receptor inhibition by the compounds and its consequence in Ca^{2+} mobilization. The intracellular calcium concentration ($[Ca^{2+}]_i$) in transfected HEK293 cells was determined at 340 nm/380 nm wavelength ratios using Fura-2 AM. Fig. 4A,B show the recordings of Ca^{2+} in HEK 293 transfected cells. Under basal conditions (without agonist or antagonist), the AT_1 receptor did not elicit any modification in intracellular Ca^{2+} concentrations. Upon Ang

II stimulation, the cells elicited a Ca^{2+} elevation with a marked peak followed by lower depletion. The injection of Ang II and Cand or ZnCand prevented Ang II-induced calcium elevation, while the complex potently reduced $[Ca^{2+}]_i$ responses. Measurement of the area under the curve (AUC) of the calcium signals was used to quantify more precisely the Ca^{2+} release (Fig. 4C and Fig. S4). The values of the AUC of the modified ligand by Zn coordination differed significantly from the Cand treatment.

Because human mesangial cells (HMC) express AT_1 receptor and elicit a contractile response in the presence of Ang II, this cell line was chosen to study the interaction of the receptor with Cand and ZnCand. The compounds did not exert toxic behavior on the HMC cells (Fig. S2). The changes in PCSA were expressed as percentages, negative control has the 0 % value, whereas Ang II (positive control) displayed the highest contraction value ca. 18.36 % after 30 min incubation. Fig. 4, D shows that ZnCand, at both concentrations, caused an inhibitory action on cell contraction induced by Ang II and there was no statistical difference in comparison to the negative control. At low concentration (0.01 µM), Cand showed no significant effect as compared to positive control and exerted less effect than ZnCand. Besides, Zn ions did not generate any effect on the contractile response of Ang II. It is important to mention that while at 0.01 µM concentrations, Zn and Cand did not exert a significant effect on the contractile action, the combined treatment of Zn + Cand should not be able to reduce the contractile effect. Taken together, these results showed that the less contractility of PCSA in the HMC cell line, induced by Ang II after incubation of the metal complex, could be assigned to a better interaction with

the AT_1 receptor due to the new structure adopted for Cand in the metal complex (see Fig. 2). Moreover, this effect could not be obtained by the combination of the antihypertensive drug (Cand) and the biometal (Zn).

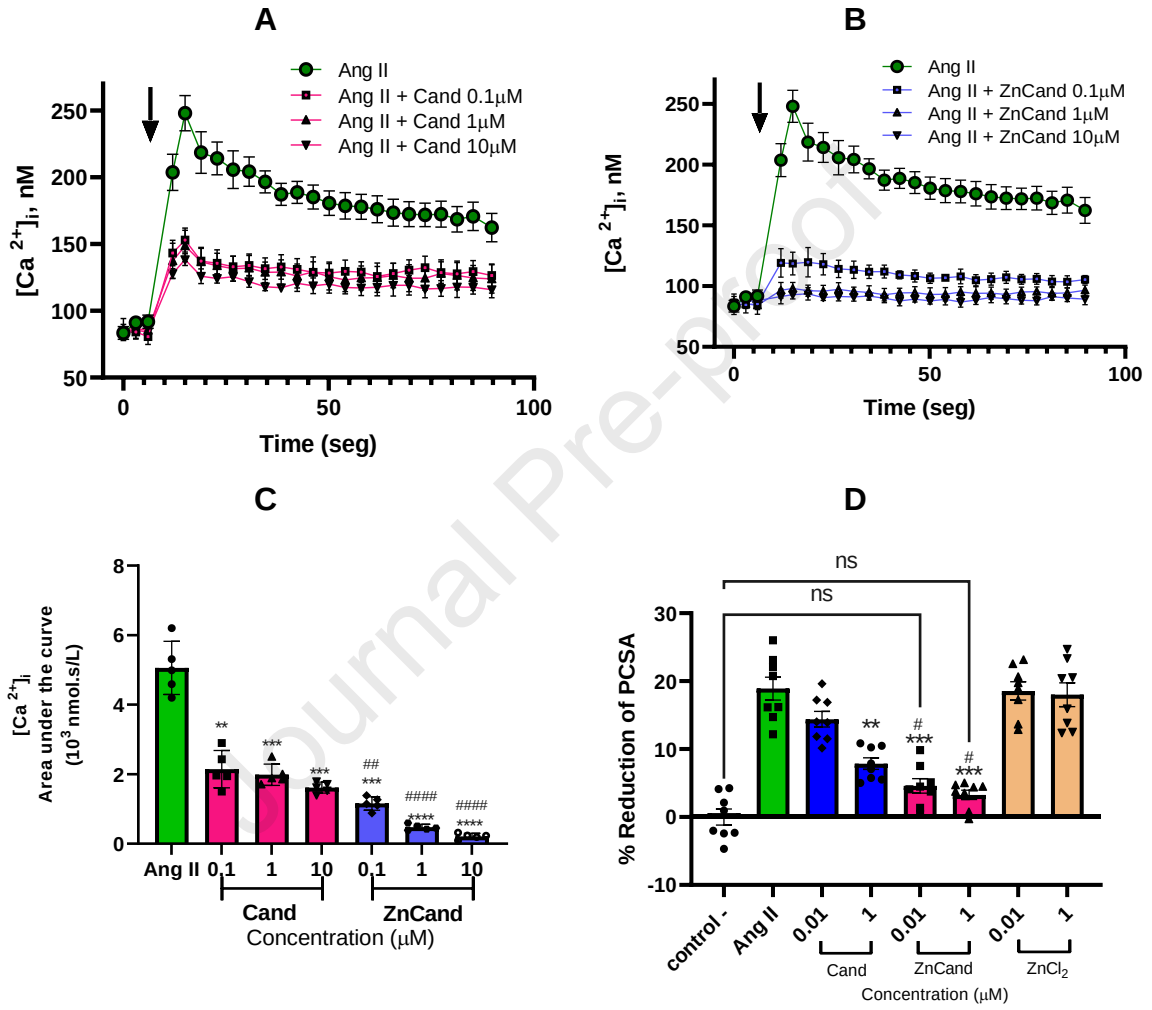

Fig. 4. Effect of Ang II alone or Ang II and candesartan (A) or ZnCand (B) on intracellular Ca^{2+} release in the HEK 293 transfected cells. Each point represents the mean ± standard error of the mean (SEM) of three independent experiments (each one performed in triplicate). Arrows indicate the injection of Ang II and Ang II plus compounds. (C) Mean values of area under curves (AUC) of calcium mobilization were obtained from the individual determinations. (D) Reduction

percentage of the planar cell surface area (PCSA), induced by AngII, in the HMC cell line after incubation with either 0.01 or 1 µM of the different compounds and subsequent addition of 1 µM Ang II. Control – (negative): cells without treatment. Control + (positive): cells treated only with 1 µM Ang II. Data are expressed as mean ± SEM. Data are expressed as mean ± SEM. (*) Values statistically significant between Cand or ZnCand and control (**p<0.01; ***p<0.001; ****p<0.0001), ($^{\#}$) Values statistically significant between Cand and ZnCand at the same concentration ($^{\#}$p<0.05,$^{\#\#}$p<0.01; $^{\#\#\#\#}$p<0.0001)

These results, together with those expressed in Fig 2, Fig 3 and Fig 4, allow us to confirm that the strategy to improve the pharmaceutical properties of Cand by structural modifications upon Zn complexation (ZnCand) produced an enhancement of the inhibition of the AT_1 receptor, leading to significant prevention of Ang II-induced ROS production, calcium fluxes, and cellular contraction.

3.3. ZnCand reduces hypertension and cardiac hypertrophy in SHR rats

To explore the antihypertensive effect of ZnCand in an *in vivo* chronic model, 3 months-old SHR male rats were treated with Cand, ZnCand or $ZnCl_2$ in the drinking water for 8 weeks. SHR-Control (untreated rats) maintained high blood pressure during the experimental period. Treatment with Cand reduced blood pressure from the second week. Rats treated with ZnCand showed a greater and statistically different effect as compared to Cand alone. As expected, $ZnCl_2$ did not show any effect during the administration (Fig 5. A).

To evaluate the effect of these compounds on heart geometry and function, the cardiac dimensions and fractional shortening were measured by echocardiography at the beginning and the end of the experimental protocol and the delta (Δ final – initial) was analyzed. The results show that, in the untreated group, interventricular septum (Δ IVSd) and the posterior wall thickness (Δ PWd) during diastole were significantly enhanced, whereas ZnCand treatment markedly prevented the increase of these parameters. Additionally, cardiac contractile function estimated by the fractional shortening was decreased in the control group at the end of the protocol, and this systolic dysfunction was prevented by ZnCand treatment. Therefore, ZnCand treatment was able to prevent hypertrophic worsening and improve systolic function in SHR rats more effectively than Cand alone (Fig. 5, C).

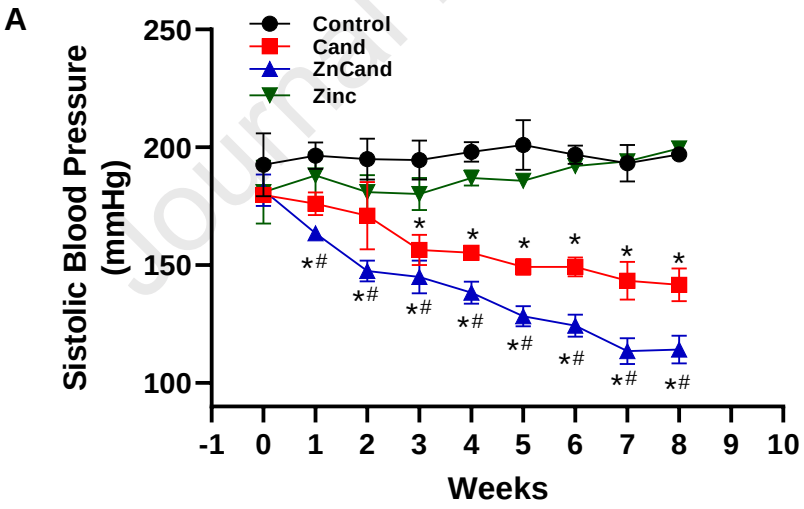

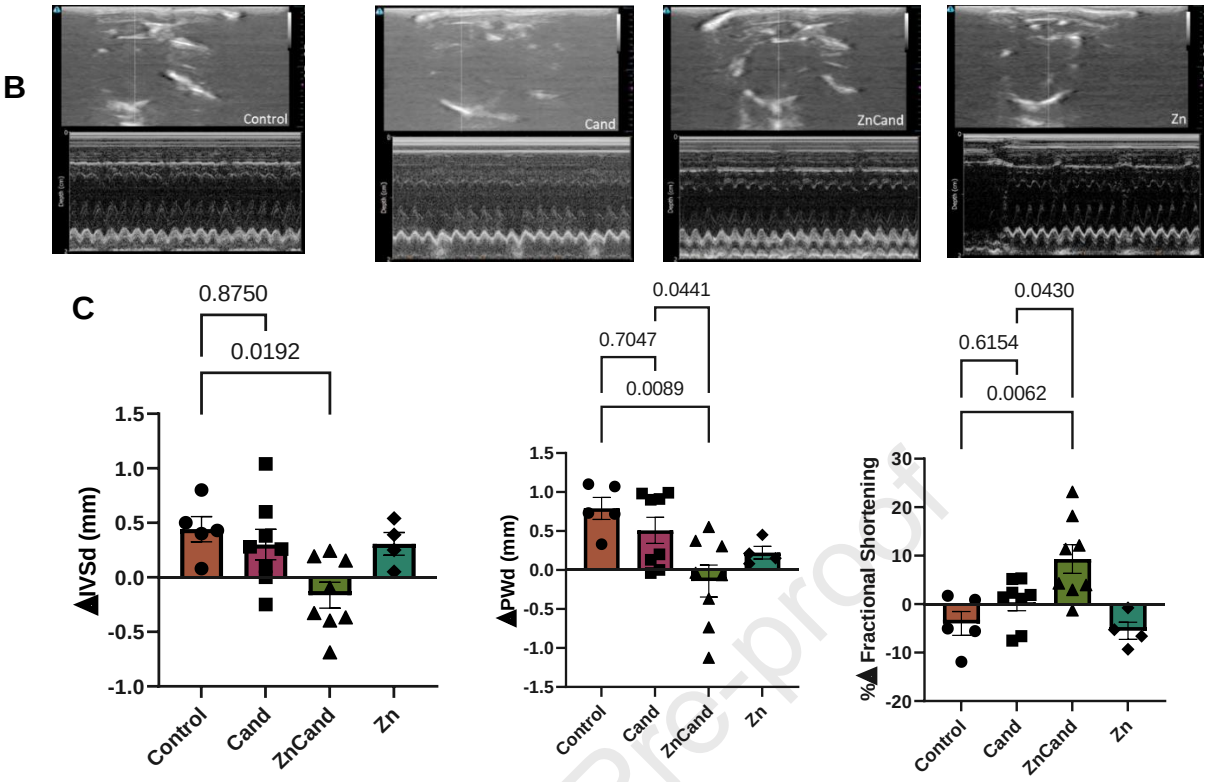

Fig. 5. (A) . Effect of ZnCand, Cand and $ZnCl_2$ on the systolic blood pressure on SHR rats, measured by the tail-cuff method. (B) Representative transthoracic echocardiography images at the end of the protocol. (C) Echocardiographic parameters were determined at the beginning of the experiment and after 8 weeks of treatment with Cand and ZnCand. Delta values are present as the mean ± SEM. Three echocardiographic images were taken from each animal. IVSd: intraventricular septum in diastole; PWd: posterior wall thickness. (*) Values statistically significant between Cand or ZnCand and control (*$p<0.05$), ($^{\#}$) Values statistically significant between Cand and ZnCand at the same concentration ($^{\#}p<0.05$)

At the end of the protocol, the cardiac hypertrophy parameters were determined. The left ventricular mass index (LVMI), calculated as the ratio LVM/BW (mg/g) and the

left ventricular mass normalized by tibia length ratio (LMV/TL) were measured. ZnCand significantly reduced the LVMI and LVM/TL as compared to untreated rats (

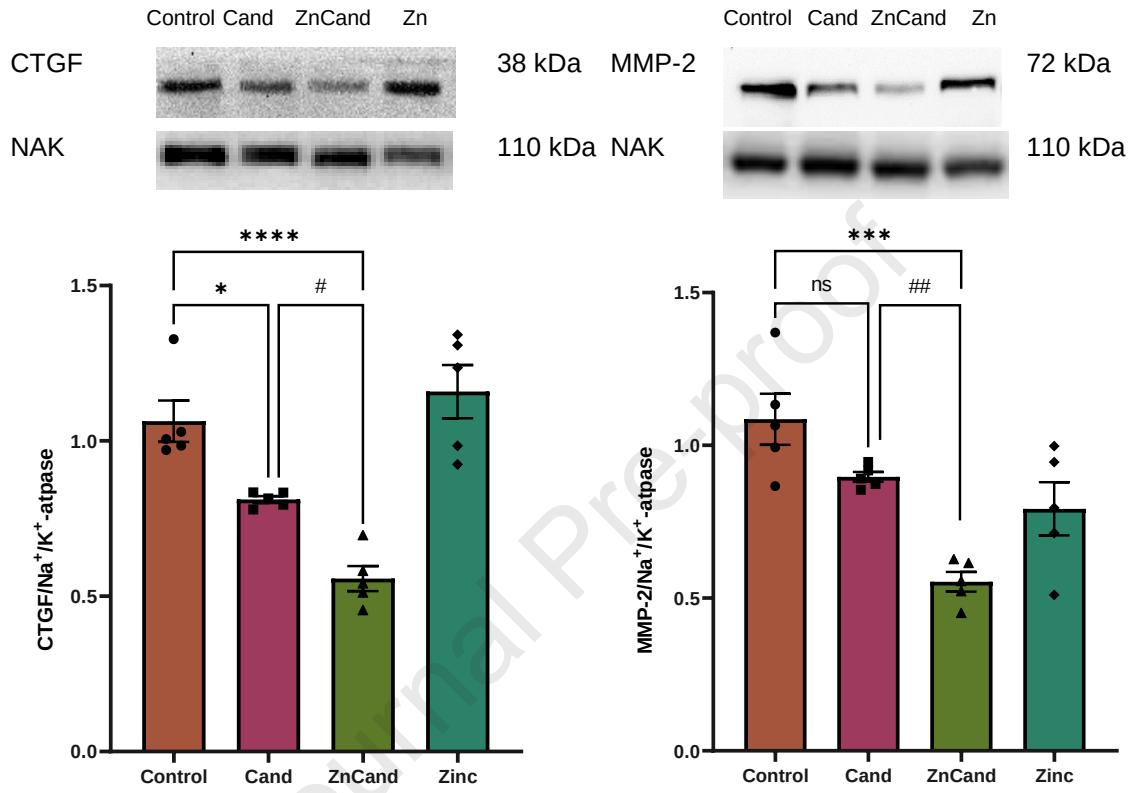

Fig. 6A,B). Histological analysis of left ventricular tissues showed an increase in cross-sectional area (CSA) of cardiomyocytes belonging to control SHR rats whereas ZnCand prevented such increment (Fig. 6C). Moreover, the percentage of interstitial type I collagen, strongly related to cardiac fibrosis, in no treated animals as well as in Zn treated rats had the highest value among groups and, Cand and ZnCand treatment reduced it being the ZnCand more efficient. (Fig. 6D, F). To confirm this histological result, the mRNA levels of the hypertrophic marker brain natriuretic peptide type B (BNP) were measured. As expected, SHR treated with

ZnCand exhibited reduced values in comparison with Cand alone or non-treated rats (Fig. 6, E).

For a better understanding of the anti-fibrotic proprieties of ZnCand, we measured the protein expression of the connective tissue growth factor (CTGF), a profibrotic factor which is strongly induced in the hypertrophic and failing heart (Dorn et al., 2018) and the matrix metalloproteinase 2 (MMP-2), a constitutive gelatinase for regulating the extracellular matrix and its higher levels in the heart is sufficient to induce ventricular dysfunction, with cardiomyocyte hypertrophy, contractile protein lysis and cardiac fibrosis(Bergman et al., 2007)

As shown in Fig. 6,G, as expected, the CTGF expression and the MMP-2 levels were found upregulated in SHR rats. Both Cand and ZnCand decreased the CTGF and MMP-2 secretions. However, treatment with ZnCand significantly prevented both proteins increment. The protein expressions were not altered in zinc group.

Taken together, these results supported that ZnCand is more effective to regress cardiac hypertrophy than the parental drug.

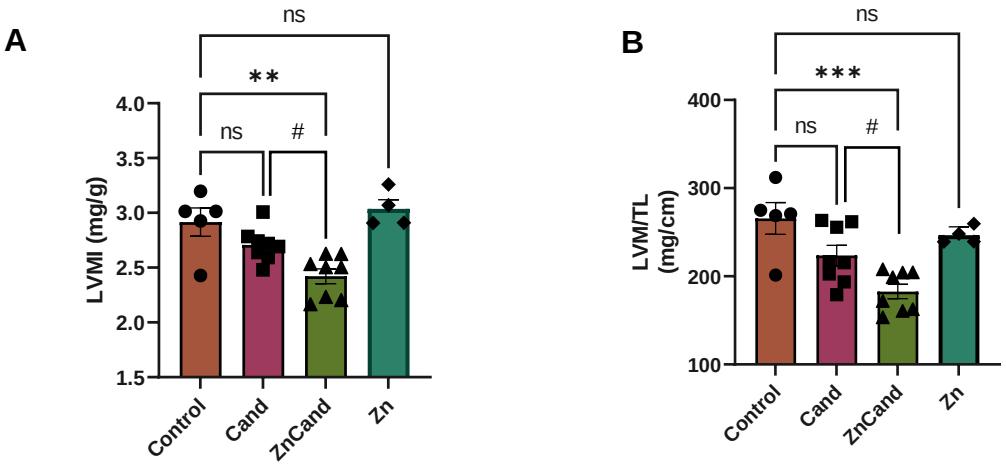

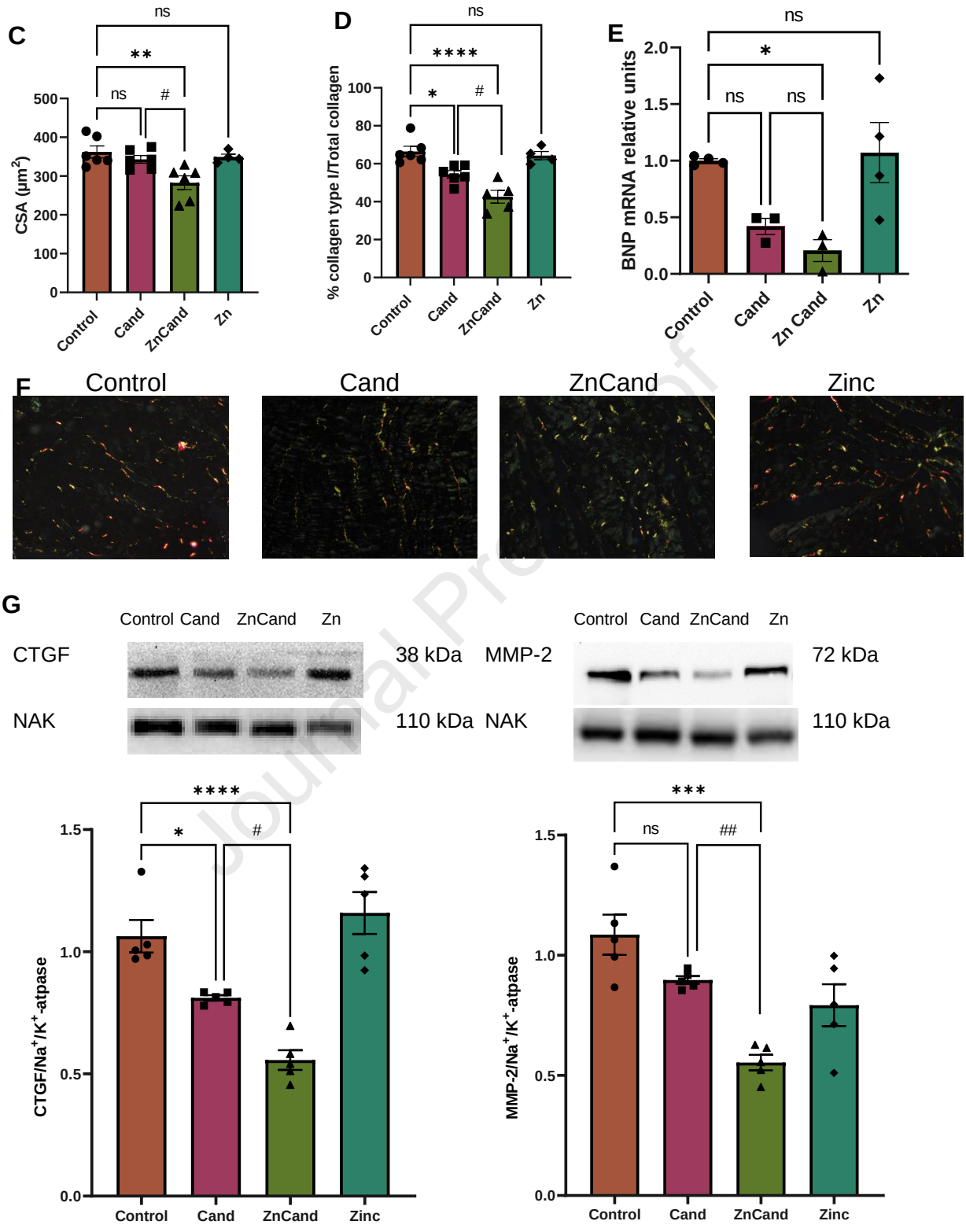

Fig. 6. Cardiac hypertrophy is estimated by the left ventricular mass index (LVMI) (ratio LVM/BW (mg/g)) (A) and left ventricular mass normalized by tibia length ratio (LVM/TL) (B). Mean values of cross-sectional area (CSA) (C), percentage of type I collagen (D) and brain natriuretic peptide type B (BNP) (E). (F) Representative images of Picrosirius red staining, type I collagen fibers appear bright and red-yellow, in sharp contrast to type III collagen which appears green. (G) Western blotting of CTGF and MMP-2 protein expression. Data are expressed as mean ± SEM. (*) Values statistically significant between Cand or ZnCand and control (*p<0.05, **p<0.01; ***p<0.001; ****p<0.0001), ($^{\#}$) Values statistically significant between Cand and ZnCand at the same concentration ($^{\#}$p<0.05; $^{\#\#}$p<0.001)

3.4. ZnCand attenuates ROS, restores the redox balance and prevents impaired Ca^{2+} handling

Hypertrophic signaling pathways are potentially modulated by ROS. Sustained Ang II stimulation, activates NADPH oxidase 2 (NOX2), the most important source of ROS in cardiomyocytes (Lambeth, 2004), which produces oxidative modifications of proteins involved in excitation-contraction coupling and alters its function. This condition leads to cytosolic Ca overload contributing to the development of contractile dysfunction (Wagner et al., 2013).

To explore the beneficial effect of ZnCand on oxidative stress, we fluorometrically quantified ROS production and glutathione redox status in left ventricular homogenates (Fig. 7). The results showed that untreated SHR heart had higher myocardial ROS production and disturbed glutathione redox status, whereas the

ZnCand treatment inhibited ROS generation, and this inhibition was associated with an increase in GSH and a decrease in GSSG.

To elucidate the mechanisms involved in ROS generation, we analyzed the expression of the catalytic NOX2 (gp91^{phox} and p47^{phox} subunits) and the cytosolic superoxide dismutase (SOD1) by Western blot. As shown in Fig. 7E, a greater level of gp91^{phox}, p47^{phox} were expressed in non-treated and zinc-treated SHR rats. Both Cand and ZnCand abolished this increase, there being a significant difference between the treatments. SOD1 expression was significantly higher in the ZnCand-treated SHR than in the Cand-treated SHR and was attenuated in the control and Zinc group.

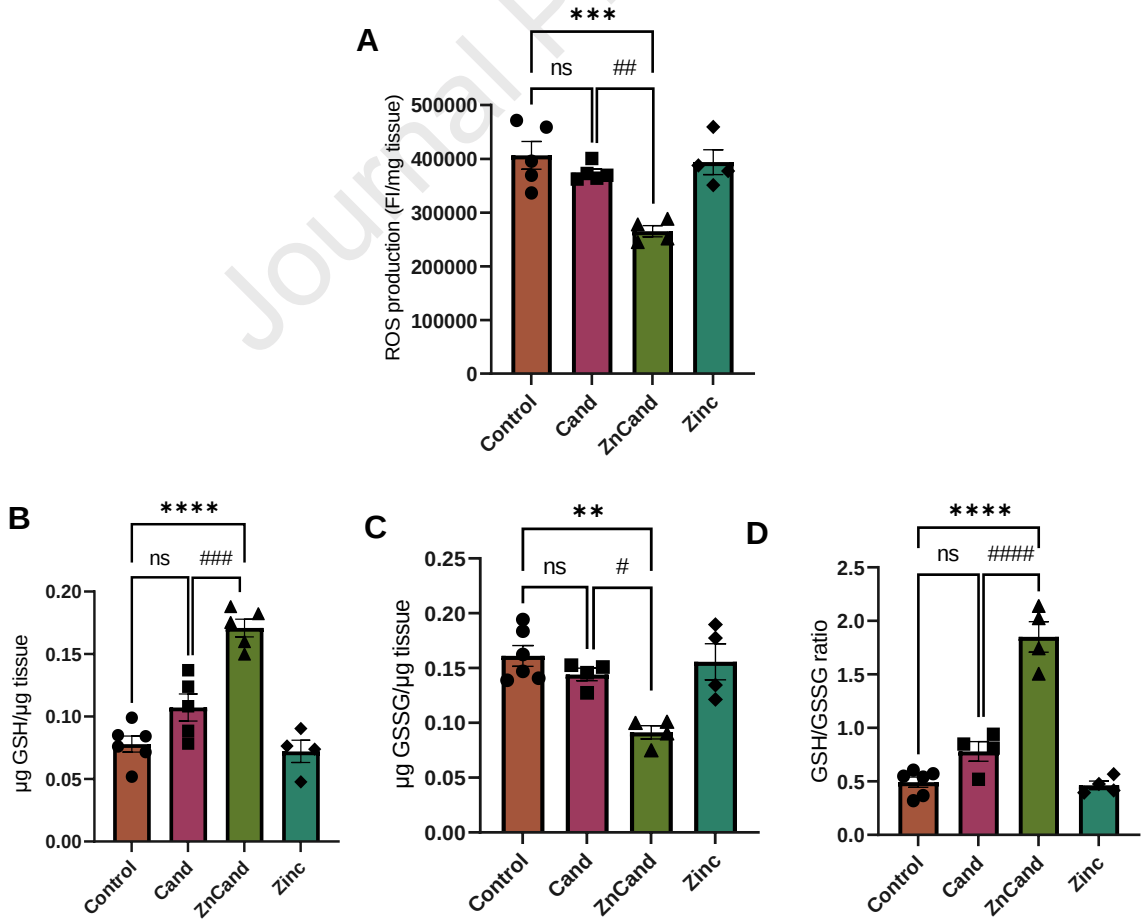

E

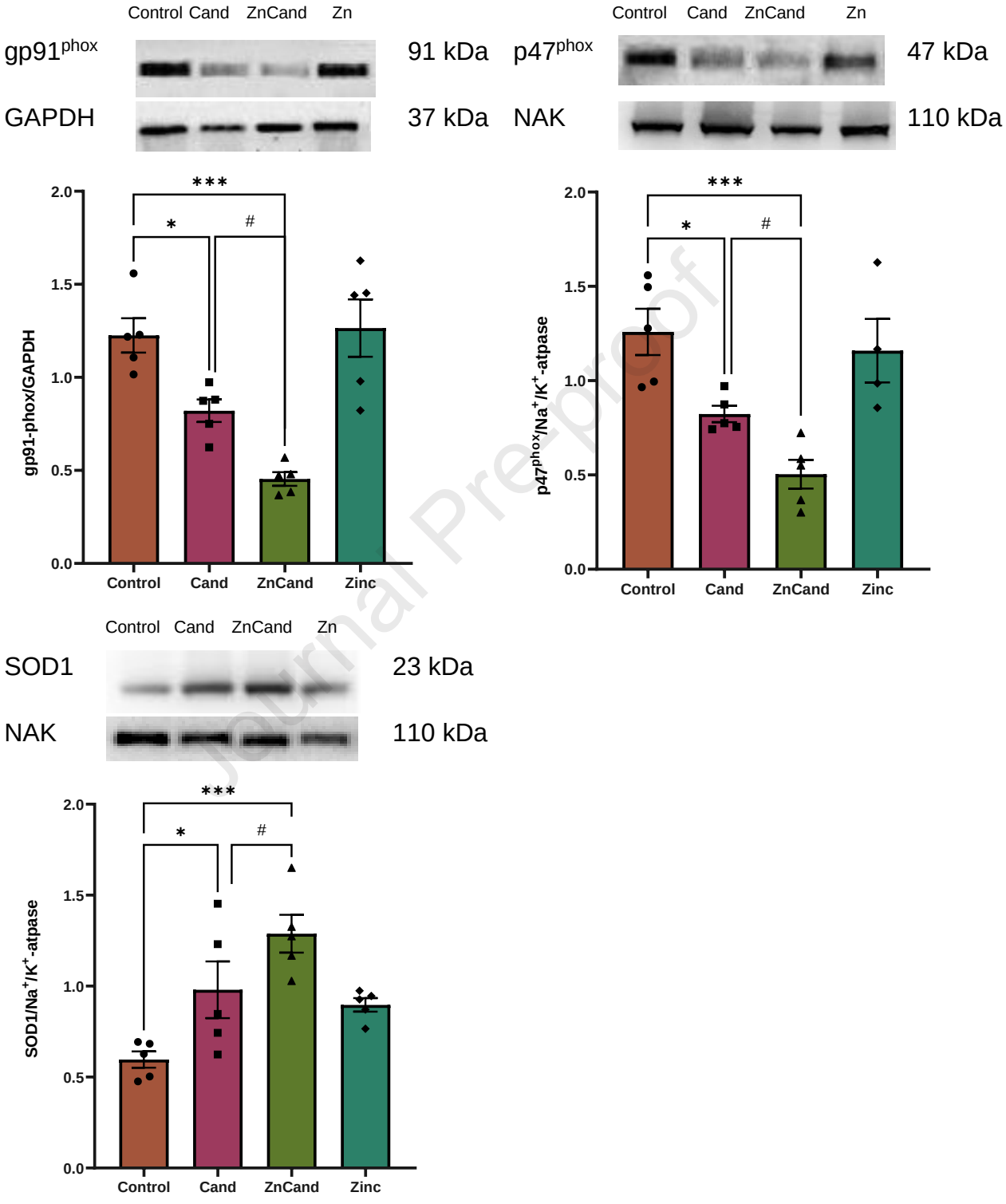

Fig. 7. Oxidative stress determination. (A) ROS production was measured by an H_2DACFDA probe and normalized by mg of tissue (FI/mg tissue). (B) and (C) GSH and GSSG determination. (D) GSH/GSSG ratio. (E) Western blotting of $gp91^{phox}$ and $p47^{phox}$ subunits and SOD1 expression. Data are expressed as mean ± SEM. (*) Values statistically significant between Cand or ZnCand and control (**p<0.01; ***p<0.001; ****p<0.0001), ($^{\#}$) Values statistically significant between Cand and ZnCand at the same concentration ($^{\#}$p<0.05; $^{\#\#}$p<0.01; $^{\#\#\#\#}$p<0.0001)

In Fig. 8A,B the amplitude of Ca^{2+} transients are shown. The ZnCand group tended to be lower than in the Cand group. No changes were observed in the amplitude of Ca^{2+} transients of Control and Zn group. Next, the dependency of ROS production and Ca^{2+} transient was assessed in isolated cardiomyocytes. Again, as mentioned earlier, ZnCand treatment diminished the oxidative stress more effective than Cand. Thus, the combination of Zn with candesartan by preventing the oxidative damage, regulates the calcium handling in cardiomyocytes.

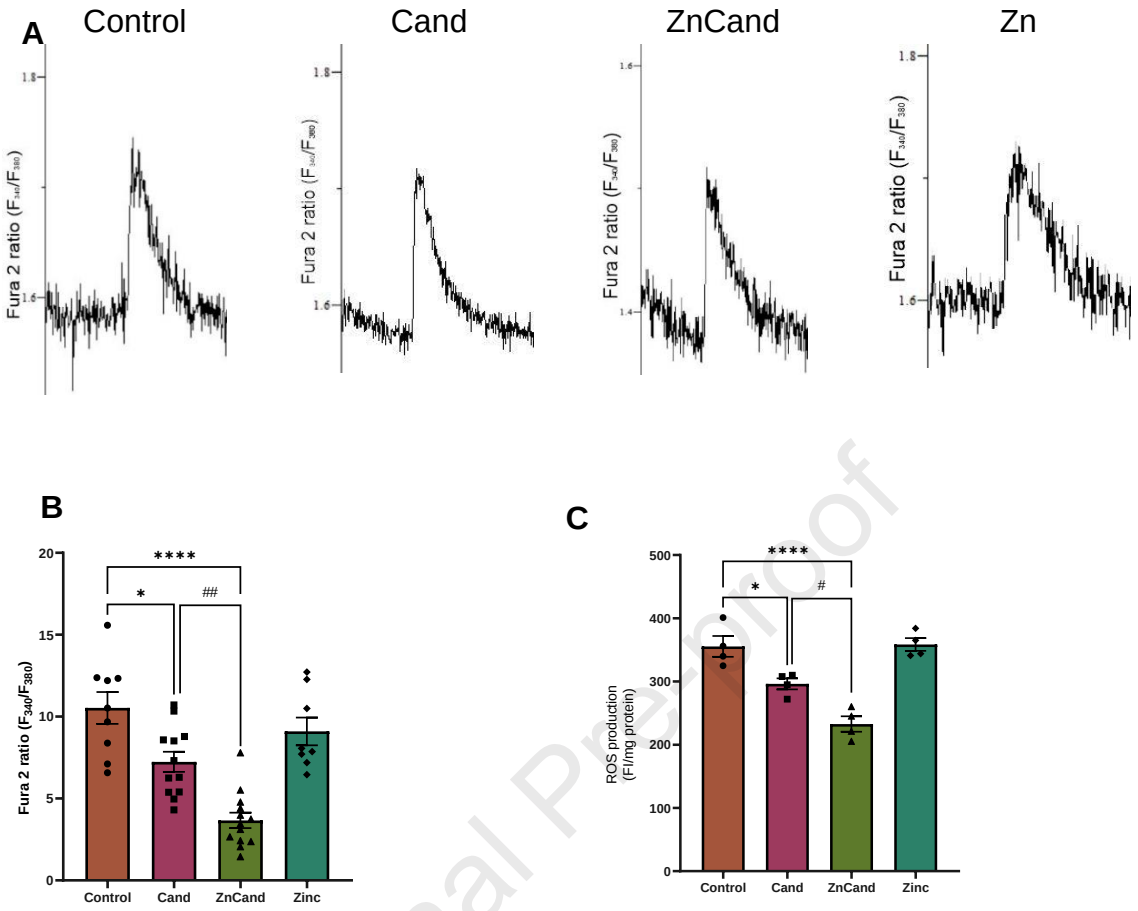

Fig. 8. (A) Representative recordings myocyte calcium (Ca^{2+}) transients (fura-2 fluorescence signal excited by 340 nm (F340)/fluorescence signal excited by 380 nm (F380)). (B) Bar graphs showing the averaged data of the parameters of Ca^{2+} transients and (C), ROS generation in left ventricular cardiomyocytes. Data are expressed as mean ± SEM. (Control, n=9 cells/3 rats; Cand, n=12/4; ZnCand, n=13/4; Zinc, n=8/3). Values statistically significant between Cand or ZnCand and control (*p<0.05; ****p<0.0001), ($^{\#}$) Values statistically significant between Cand and ZnCand at the same concentration ($^{\#}$p<0.05)

4. Discussion

The main finding of the present work is that the designed compound, ZnCand, a coordination complex synthesized between the ARB Candesartan and Zn(II), is a stronger antagonist of the AT_1 receptor, preventing its activation more effectively than the parent drug (Cand), thus, reducing the oxidative stress, attenuating calcium response and cell contraction. Moreover, *in vivo* experiments showed that ZnCand, at candesartan molar equivalent doses, reduced systolic arterial pressure and led to regression of left ventricular hypertrophy and cardiac fibrosis.

Many of the physiological, as well as pathological cardiovascular functions, are mediated mostly *via* the renin-angiotensin system (RAS) where the Ang II acts through the AT_1 receptor and the AT_2 receptor (Singh and Karnik, 2020). The increased levels of Ang II and the overactivation of the AT_1 receptor, resulting in vasoconstriction, growth in myocytes, left ventricular hypertrophy and progressive myocardial remodeling and dysfunction, are responsible for heart failure (Arumugam et al., 2016). Angiotensin II receptor, type 1 blockers (ARB) are commonly used for the treatment of hypertension and cardiovascular diseases (See, 2001). These types of antihypertensive drugs are well tolerated, reduce the left ventricular (LV) mass (Penicka et al., 2009) as well as the rate of cardiovascular events better than beta-adrenergic receptor antagonists, angiotensin-converting enzyme inhibitors (ACEI) or calcium channel blockers, due to their selective binding to AT_1 receptor (Cuspidi, 2008; Neutel and Smith, 2003). Although Candesartan is a highly selective ARB and exerts a preventive effect on cardiac hypertrophy, it resulted more effective when administrated in combination with the thiazide diuretic, hydrochlorothiazide, or ACEIs (Husain et al., 2011; McKelvie et al., 1999). Otherwise, the treatment to

suppress the ventricular remodeling, restore the ejection fraction or reduce the natriuretic peptide type B (BNP) must be recommended for long periods (Hiroshi et al., 2004). In comparison with other sartans, like olmesartan, irbesartan and azilsartan, these effects may be due to a lower affinity for AT_1 receptor of candesartan, and therefore, a lower tropism for vasculature and especially for myocardium (Tuccinardi et al., 2006). This highlights the fact that the difference of one residue in the molecular structure of the sartan-group of pharmaceuticals, modifies the bonding properties with the receptor, leading to a better interaction with the hydrophobic pocket in the AT1R (Miura et al., 2011). Indeed, the tetrazole ring in candesartan was replaced by the oxadiazole ring in azilsartan to make it less acidic and more lipophilic and to have more beneficial effects (Sakamoto et al., 2015).

To improve the pharmacological activity of candesartan, we have previously modified its structure with Zn(II), a trace element that is involved in the maintenance of cellular structure and function (Martínez et al., 2022, 2021a). In the present study, we found that the ZnCand complex produced a greater AT_1 receptor blockade probably for at least two reasons: Zn(II) binds to one oxygen atom from the carboxylate group and the N atom from the tetrazole group (Martínez et al., 2021a) inducing a conformational change in candesartan which lead into increased association with AT_1 receptor. Additionally, the complexation provokes changes in the hydrophobicity of the molecule allowing the interaction with the hydrophobic pocket of the receptor. Predicted data propose that the hydrophobic interaction and π-π contacts could contribute to the high potency of the drug to AT_1 receptor (Zhang et al., 2015).

The stimulation of the AT_1 receptor by Ang II is linked to the activation of an NADH/NADPH oxidase, which is the major source of ROS in vascular cells (Nguyen Dinh Cat et al., 2013). ROS enhances the vascular $[Ca^{2+}]_i$ by stimulating inositol trisphosphate-mediated Ca^{2+} mobilization, by increasing cytosolic Ca^{2+} through sarcoplasmic/endoplasmic reticulum Ca^{2+}-ATPase inhibition, and by stimulating Ca^{2+} influx through Ca^{2+} channels, thereby altering vascular contractility and tone which cause cellular dysfunction (Negri et al., 2021)(Touyz, 2005). Thus, interfering in cellular ROS production and Ca^{2+} release could restore cardiovascular disorders. This response can be studied in HEK 293 cells transfected with the AT_1 receptor (Bernhem et al., 2017). The metallodrug ZnCand generated a reduction in ROS production, leading to attenuation in calcium signaling more effectively than candesartan alone. Additionally, this effect could be observed in mesangial cells, where incubation of ZnCand, under Ang II stimulation, prevented cell contraction. Previous findings showed that Ang II exerted a synergistic effect on ROS production. Thus, the prevention of RAS activation by blocking the AT_1 receptor could generate the inhibition of the mesangial oxidative stress with the decrease of the contractile response (Akaishi et al., 2019; Torrecillas et al., 2001). So far, we have shown in *in vitro* studies*,* that the structural modification of candesartan with Zn(II) improves the AT_1 blockade, inhibited ROS generation, and reduced calcium influx, which leads to a less contractile response.

RAS overactivation is related to the development and progression of hypertension and heart failure. The sustained increase in blood pressure imposes a chronic workload on the heart and the left ventricular mass hypertrophies as a maladaptive response (Kahan, 2005). Moreover, the direct effect of Ang II on cardiomyocytes

growth (Arumugam et al., 2016), ROS production, the proliferation and differentiation of cardiac fibroblasts, by activating TGF-*β* (transforming growth factor *β*) and mitogen-activated protein kinases (MAPKs) pathways and on the synthesis of extracellular matrix and its regulation through the MMPS and CTGF to form myocardial fibrosis (Li et al., 2015)(Arenas et al., 2004), contributes to LV myocardial remodeling. The successful management of high blood pressure by the inhibition of the pressor arm of RAS modifies this response and produces regression of LVH (Soliman et al., 2017). Our work revealed that, after eight weeks of treatment, ZnCand produced a greater lowering blood pressure than its parental drug. The blood pressure decrease was positively correlated with the attenuation of cardiac hypertrophy, indicating that by lowering the blood pressure, the peripheral resistance and impedance for ventricular emptying decreases, reducing the pressure overload and reversing LVH. Additionally, the gene expression of hypertrophic marker BNP, stimulated by Ang II and a powerful predictor of LV dysfunction (Kuwahara, 2021), was significantly downregulated in treated rats, indicating the improvement of cardiac function. Moreover, a better blocking of the AT_1 receptor by ZnCand, represses the CTGF signaling and modulates the MMP-2 expression, which might explain its anti-fibrotic properties(Yu et al., 2012).

Although the mechanical stress declines, the compound could have had a direct effect on cardiomyocytes due to the strong binding to the AT_1 receptor and this cardioprotection provoked by ZnCand could occur at least, in part, *via* the NOX inhibition, which suppresses the oxidative stress and restores the redox homeostasis. Together with the upregulation of SOD1 by ZnCand promotes a great antioxidant defense system. Likewise, a powerful oxidative stress reductions

declines the intracellular calcium concentration and restores the contractile functions. Additionally, ZnCand exerts a dual function on the mitigation of fibrotic mediators, which not only could be repressed by AT1 receptor blockade, but also by attenuation of oxidative damage (Gonçalves et al., 2022; Wong et al., 2018).

In the light of these findings, the present study supports that this metallodrug normalizes the blood pressure and restores the cardiac function more effectively than its parenteral drug. These promising results would indicate that ZnCand should have the potential to be the treatment in terms of CV protection for patients with hypertensive heart disease, avoiding the need to implement multi-drug treatments.

Author statement

Declaration of Competing Interest: None.

Acknowledgments: The authors thank to Leandro Di Cianni for the technical support to measure the blood pressure and Rodrigo Da Silva for his help in the execution of the binding experiment. This work was supported by UNLP (X871, V270), CICPBA, and ANPCyT (PICT 2019-0945, 2019-0206), Argentina. and EGF are members of the Research Career, CONICET, Argentina. VRM is fellowship holder from CONICET. JOVR is a research career member of UNLP. MSI, ELP, VDG, CJDG and EGF are research career members of CONICET. PAMW is member of the Research Career, CICPBA.

Supplementary data: Fig S1. Viability of transfected HEK293 cells treated with Cand and ZnCand for 90 min. Each result (performed in triplicate) represents the mean ± standard error of the mean (SEM) of three independent experiments. Cell viability was calculated as the percentage of live cells compared to no treated cells (% control). ****Statistically significant values between Ang II-treated cells and control ($p < 0.001$). Fig S2. Flow cytometry in human mesangial cells (HMC) dyed with both iodide propidium (IP, in FL3) and H_2DCFDA (for intracellular ROS, in FL1). a-i) Dotplots FL1-H vs FL3-H after 24 h of treatment with Cand (a,d), ZnCand (b,e), $Zn(NO_3)_2$ (c,f) at 50 μM or 100 μM in DMSO 0.5% and controls: without previous treatment (g), with 0.5% of DMSO (h), and i) with Tert-Butyl hydroperoxide (TBHP, 100 μM) a ROS positive control. j,k) Overlapped histograms in FL1-H (ROS sensitive) after treatment with 50 μM (j) or 100 μM (k) of Cand (in red), ZnCand (in blue), $Zn(NO_3)_2$ (in green) and control with DMSO (in black). In every dotplot the quadrants are named: LL (lower-left, IP-/ ROS-), UL (upper-left, IP-/ROS+), UR (upper-right, IP+/ROS+), LR (lower-right, IP+/ROS-). l-o) Percentage average cell population in every quadrant for each treatment at 50 μM (in black) and 100 μM (in gray) error expressed as ± SEM (n=3), only TBHP (ROS+ control) has shown statistically differences with control ($p < 0.05$). Fig. S3: representative confocal images of transient transfected HEK293 cells expressing YFP-tagged AT_1 receptor (yellow) and nucleus stained with DAPI (blue) treatead with Ang II TAMRA and Ang II TAMRA+ Ang II salt. Fig. S4. Effect of Ang II on intracellular Ca^{2+} release in the HEK 293 transfected cells. Plot showing the calculated area under the curve.

References

Akaishi, T., Abe, M., Okuda, H., Ishizawa, K., Abe, T., Ishii, T., Ito, S., 2019. High glucose level and angiotensin II type 1 receptor stimulation synergistically amplify oxidative stress in renal mesangial cells. Sci Rep 9, 5214–5221. https://doi.org/10.1038/s41598-019-41536-z

Arenas, I.A., Xu, Y., Lopez-Jaramillo, P., Davidge, S.T., 2004. Angiotensin II-induced MMP-2 release from endothelial cells is mediated by TNF-α. Am J Physiol Cell Physiol 286. https://doi.org/10.1152/ajpcell.00398.2003

Aronow, W.S., 2017. Hypertension and left ventricular hypertrophy. Ann Transl Med 5, 1–4. https://doi.org/10.21037/atm.2017.06.14

Arumugam, S., Sreedhar, R., Thandavarayan, R.A., Karuppagounder, V., Krishnamurthy, P., Suzuki, K., Nakamura, M., Watanabe, K., 2016. Angiotensin receptor blockers: Focus on cardiac and renal injury. Trends Cardiovasc Med 26, 221–228. https://doi.org/10.1016/j.tcm.2015.06.004

Bergman, M.R., Teerlink, J.R., Mahimkar, R., Li, L., Zhu, B.Q., Nguyen, A., Dahi, S., Karliner, J.S., Lovett, D.H., 2007. Cardiac matrix metalloproteinase-2 expression independently induces marked ventricular remodeling and systolic dysfunction. Am J Physiol Heart Circ Physiol 292. https://doi.org/10.1152/ajpheart.00434.2006

Bernhem, K., Krishnan, K., Bondar, A., Brismar, H., Aperia, A., Scott, L., 2017. AT1-receptor response to non-saturating Ang-II concentrations is amplified by calcium channel blockers. BMC Cardiovasc Disord 17, 126–136. https://doi.org/10.1186/s12872-017-0562-x

Bradford, M.M., 1976. A rapid and sensitive method for the quantitation of microgram quantities of protein utilizing the principle of protein-dye binding. Anal Biochem 72, 248–254. https://doi.org/10.1016/0003-2697(76)90527-3

Bragina, M., Stergiopulos, N., Fraga-Silva, R., 2017. Fluorescence-Based Binding Assay for Screening Ligands of Angiotensin Receptors, in: The Renin-Angiotensin-Aldosterone System. Methods and Protocols. pp. 165–174.

Brown, L., Fenning, A., Shek, A., Burstow, D., 2001. Reversal of cardiovascular remodelling with candesartan. Journal of the Renin-Angiotensin-Aldosterone System 2, S141–S147. https://doi.org/10.1177/14703203010020012501

Bruijnincx, P.C., Sadler, P.J., 2008. New trends for metal complexes with anticancer activity. Curr Opin Chem Biol 12, 197–206. https://doi.org/10.1016/j.cbpa.2007.11.013

Choi, H., Leto, T.L., Hunyady, L., Catt, K.J., Bae, Y.S., Rhee, S.G., 2008. Mechanism of Angiotensin II-induced Superoxide Production in Cells Reconstituted with Angiotensin Type 1 Receptor and the Components of NADPH Oxidase. Journal of Biological Chemistry 283, 255–267. https://doi.org/10.1074/jbc.M708000200

Cuspidi, C., 2008. Angiotensin II receptor blockers and cardiovascular protection: Focus on left ventricular hypertrophy regression and atrial fibrillation prevention. Vasc Health Risk Manag 4, 67–73. https://doi.org/10.2147/vhrm.2008.04.01.67

Devereux, R.B., Reichek, N., 1977. Echocardiographic determination of left ventricular mass in man. Anatomic validation of the method. Circulation 55, 613–618. https://doi.org/10.1161/01.CIR.55.4.613

Dorn, L.E., Petrosino, J.M., Wright, P., Accornero, F., 2018. CTGF/CCN2 is an autocrine regulator of cardiac fibrosis. J Mol Cell Cardiol 121. https://doi.org/10.1016/j.yjmcc.2018.07.130

Gonçalves, P.R., Nascimento, L.D., Gerlach, R.F., Rodrigues, K.E., Prado, A.F., 2022. Matrix Metalloproteinase 2 as a Pharmacological Target in Heart Failure. Pharmaceuticals. https://doi.org/10.3390/ph15080920

Gradman, A.H., Alfayoumi, F., 2006. From Left Ventricular Hypertrophy to Congestive Heart Failure: Management of Hypertensive Heart Disease. Prog Cardiovasc Dis 48, 326–341. https://doi.org/10.1016/j.pcad.2006.02.001

Grießner, M., Bröker, P., Lehmann, A., Ehrentreich-Förster, E., Bier, F.F., 2009. Detection of angiotensin II type 1 receptor ligands by a cell-based assay. Anal Bioanal Chem 395, 1937–1940. https://doi.org/10.1007/s00216-009-3074-4

Grynkiewicz, G., Poenie, M., Tsien, R.Y., 1985. A new generation of Ca^{2+} indicators with greatly improved fluorescence properties. Journal of Biological Chemistry 260, 3440–3450. https://doi.org/3838314

Hiroshi, S., Ryuji, S., Hideki, N., Yoshitaka, I., Takeshi, K., Hitoshi, E., Yuji, H., Shinji, K., Eiichi, G., Takahsi, K., 2004. Candesartan successfully prevents left ventricular remodeling after myocardial infarction. J Card Fail 10, S181. https://doi.org/10.1016/j.cardfail.2004.08.108

Hissin, P.J., Hilf, R., 1976. A fluorometric method for determination of oxidized and reduced glutathione in tissues. Anal Biochem 74, 214–226. https://doi.org/10.1016/0003-2697(76)90326-2

Husain, A., Azim Md Sabir, M.S., Mitra, M., Bhasin, P.S., 2011. A review on Candesartan: Pharmacological and pharmaceutical profile. J Appl Pharm Sci.

Inuzuka, T., Fujioka, Y., Tsuda, M., Fujioka, M., Satoh, A.O., Horiuchi, K., Nishide, S., Nanbo, A., Tanaka, S., Ohba, Y., 2016. Attenuation of ligand-induced activation of angiotensin II type 1 receptor signaling by the type 2 receptor via protein kinase C. Sci Rep 6, 21613. https://doi.org/10.1038/srep21613

Islas, M.S., Luengo, A., Franca, C. a., Merino, M.G., Calleros, L., Rodriguez-Puyol, M., Lezama, L., Ferrer, E.G., Williams, P. a. M., 2016. Experimental and DFT characterization, antioxidant and anticancer activities of a Cu(II)–irbesartan complex: structure–antihypertensive activity relationships in Cu(II)–sartan complexes. Journal of Biological Inorganic Chemistry 21, 851–863. https://doi.org/10.1007/s00775-016-1384-5

Jones, E.F., Harrap, S.B., Calafiore, P., Tonkin, A.M., 1992. Development and validation of echocardiography methods for estimating left ventricular mass in rats. Clin Exp Pharmacol Physiol 19, 361–364. https://doi.org/10.1111/j.1440-1681.1992.tb00472.x

Kahan, T., 2005. Left ventricular hypertrophy in hypertension: its arrhythmogenic potential. Heart 91, 250–256. https://doi.org/10.1136/hrt.2004.042473

Kuwahara, K., 2021. The natriuretic peptide system in heart failure: Diagnostic and therapeutic implications. Pharmacol Ther 227, 107863. https://doi.org/10.1016/j.pharmthera.2021.107863

Lambeth, J.D., 2004. NOX enzymes and the biology of reactive oxygen. Nat Rev Immunol. https://doi.org/10.1038/nri1312

Li, R., Xiao, J., Qing, X., Xing, J., Xia, Y., Qi, J., Liu, X., Zhang, S., Sheng, X., Zhang, X., Ji, X., 2015. Sp1 Mediates a Therapeutic Role of MiR-7a/b in Angiotensin II-Induced Cardiac Fibrosis via Mechanism Involving the TGF-β

and MAPKs Pathways in Cardiac Fibroblasts. PLoS One 10, e0125513. https://doi.org/10.1371/journal.pone.0125513

Louch, W.E., Sheehan, K.A., Wolska, B.M., 2011. Methods in cardiomyocyte isolation, culture, and gene transfer. J Mol Cell Cardiol. https://doi.org/10.1016/j.yjmcc.2011.06.012

Martínez, V.R., Aguirre, M. v, Todaro, J.S., Ferrer, E.G., Williams, P.A.M., 2021a. Candesartan and valsartan Zn(II) complexes as inducing agents of reductive stress: mitochondrial dysfunction and apoptosis. New Journal of Chemistry 45, 939–951. https://doi.org/10.1039/D0NJ02937H

Martínez, V.R., Aguirre, M. v, Todaro, J.S., Lima, A.M., Stergiopulos, N., Ferrer, E.G., Williams, P.A., 2021b. Zinc complexation improves angiotensin II receptor type 1 blockade and *in vivo* antihypertensive activity of telmisartan. Future Med Chem 13, 13–23. https://doi.org/10.4155/fmc-2020-0093

Martínez, V.R., Ferrer, E.G., Williams, P.A., 2022. Candesartan, losartan and valsartan Zn(II) complexes interactions with bovine serum albumin. Future Med Chem 14, 9–16. https://doi.org/10.4155/fmc-2021-0216

McKelvie, R.S., Yusuf, S., Pericak, D., Avezum, A., Burns, R.J., Probstfield, J., Tsuyuki, R.T., White, M., Rouleau, J., Latini, R., Maggioni, A., Young, J., Pogue, J., 1999. Comparison of Candesartan, Enalapril, and Their Combination in Congestive Heart Failure. Circulation 100, 1056–1064. https://doi.org/10.1161/01.CIR.100.10.1056

Miura, S.I., Karnik, S.S., Saku, K., 2011. Angiotensin II type 1 receptor blockers: class effects versus molecular effects. JRAAS - Journal of the Renin-

Angiotensin-Aldosterone System 12, 1–7. https://doi.org/10.1177/1470320310370852

Mjos, K.D., Orvig, C., 2014. Metallodrugs in medicinal inorganic chemistry. Chem Rev 114, 4540–4558. https://doi.org/10.1021/cr400460s

Montezano, A.C., Nguyen Dinh Cat, A., Rios, F.J., Touyz, R.M., 2014. Angiotensin II and Vascular Injury. Curr Hypertens Rep 16, 431–442. https://doi.org/10.1007/s11906-014-0431-2

Mousavi, K., Niknahad, H., Ghalamfarsa, A., Mohammadi, H., Azarpira, N., Ommati, M.M., Heidari, R., 2020. Taurine mitigates cirrhosis-associated heart injury through mitochondrial-dependent and antioxidative mechanisms. Clin Exp Hepatol 6, 207–219. https://doi.org/10.5114/ceh.2020.99513

Negri, S., Faris, P., Moccia, F., 2021. Reactive Oxygen Species and Endothelial Ca2+ Signaling: Brothers in Arms or Partners in Crime? Int J Mol Sci 22, 9821. https://doi.org/10.3390/ijms22189821

Neutel, J.M., Smith, D.H.G., 2003. Evaluation of Angiotensin II Receptor Blockers for 24-Hour Blood Pressure Control: Meta-Analysis of a Clinical Database. The Journal of Clinical Hypertension 5, 58–63. https://doi.org/10.1111/j.1524-6175.2003.01612.x

Nguyen Dinh Cat, A., Montezano, A.C., Burger, D., Touyz, R.M., 2013. Angiotensin II, NADPH Oxidase, and Redox Signaling in the Vasculature. Antioxid Redox Signal 19, 1110–1120. https://doi.org/10.1089/ars.2012.4641

Pace, N., Weerapana, E., 2014. Zinc-Binding Cysteines: Diverse Functions and Structural Motifs. Biomolecules 4, 419–434. https://doi.org/10.3390/biom4020419

Penicka, M., Gregor, P., Kerekes, R., Marek, D., Curila, K., Krupicka, J., 2009. The Effects of Candesartan on Left Ventricular Hypertrophy and Function in Nonobstructive Hypertrophic Cardiomyopathy. The Journal of Molecular Diagnostics 11, 35–41. https://doi.org/10.2353/jmoldx.2009.080082

Sakamoto, M., Asakura, M., Nakano, A., Kanzaki, H., Sugano, Y., Amaki, M., Ohara, T., Hasegawa, T., Anzai, T., Kitakaze, M., 2015. Azilsartan, but not Candesartan Improves Left Ventricular Diastolic Function in Patients with Hypertension and Heart Failure. Int J Gerontol 9, 201–205. https://doi.org/10.1016/j.ijge.2015.06.003

See, S., 2001. Angiotensin II receptor blockers for the treatment of hypertension. Expert Opin Pharmacother 2, 1795–1804. https://doi.org/10.1517/14656566.2.11.1795

Singh, K.D., Karnik, S.S., 2020. Angiotensin Type 1 Receptor Blockers in Heart Failure. Curr Drug Targets 21, 125–131. https://doi.org/10.2174/1389450120666190821152000

Soliman, E.Z., Ambrosius, W.T., Cushman, W.C., Zhang, Z., Bates, J.T., Neyra, J.A., Carson, T.Y., Tamariz, L., Ghazi, L., Cho, M.E., Shapiro, B.P., He, J., Fine, L.J., Lewis, C.E., 2017. Effect of Intensive Blood Pressure Lowering on Left Ventricular Hypertrophy in Patients With Hypertension. Circulation 136, 440–450. https://doi.org/10.1161/CIRCULATIONAHA.117.028441

Takimoto, E., Kass, D.A., 2007. Role of Oxidative Stress in Cardiac Hypertrophy and Remodeling. Hypertension 49, 241–248. https://doi.org/10.1161/01.HYP.0000254415.31362.a7

Torrecillas, G., Boyano-Adánez, M. del C., Medina, J., Parra, T., Griera, M., López-Ongil, S., Arilla, E., Rodríguez-Puyol, M., Rodríguez-Puyol, D., 2001. The Role of Hydrogen Peroxide in the Contractile Response to Angiotensin II. Mol Pharmacol 59, 104–112. https://doi.org/10.1124/mol.59.1.104

Touyz, R.M., 2005. Reactive Oxygen Species as Mediators of Calcium Signaling by Angiotensin II: Implications in Vascular Physiology and Pathophysiology. Antioxid Redox Signal 7, 1302–1314. https://doi.org/10.1089/ars.2005.7.1302

Tuccinardi, T., Calderone, V., Rapposelli, S., Martinelli, A., 2006. Proposal of a New Binding Orientation for Non-Peptide AT1 Antagonists: Homology Modeling, Docking and Three-Dimensional Quantitative Structure−Activity Relationship Analysis. J Med Chem 49, 4305–4316. https://doi.org/10.1021/jm060338p

Virdis, A., Duranti, E., Taddei, S., 2011. Oxidative Stress and Vascular Damage in Hypertension: Role of Angiotensin II. Int J Hypertens 2011, 1–7. https://doi.org/10.4061/2011/916310

Wagner, S., Rokita, A.G., Anderson, M.E., Maier, L.S., 2013. Redox regulation of sodium and calcium handling. Antioxid Redox Signal. https://doi.org/10.1089/ars.2012.4818

Wong, C.K.S., Falkenham, A., Myers, T., Légaré, J.F., 2018. Connective tissue growth factor expression after angiotensin II exposure is dependent on transforming growth factor-β signaling via the canonical smad-dependent pathway in hypertensive induced myocardial fibrosis. JRAAS - Journal of the Renin-Angiotensin-Aldosterone System 19. https://doi.org/10.1177/1470320318759358

Yu, H., Zhao, G., Li, H., Liu, X., Wang, S., 2012. Candesartan antagonizes pressure overload-evoked cardiac remodeling through Smad7 gene-dependent MMP-9 suppression. Gene 497. https://doi.org/10.1016/j.gene.2012.01.081

Zhang, H., Unal, H., Gati, C., Han, G.W., Liu, W., Zatsepin, N.A., James, D., Wang, D., Nelson, G., Weierstall, U., Sawaya, M.R., Xu, Q., Messerschmidt, M., Williams, G.J., Boutet, S., Yefanov, O.M., White, T.A., Wang, C., Ishchenko, A., Tirupula, K.C., Desnoyer, R., Coe, J., Conrad, C.E., Fromme, P., Stevens, R.C., Katritch, V., Karnik, S.S., Cherezov, V., 2015. Structure of the Angiotensin Receptor Revealed by Serial Femtosecond Crystallography. Cell 161, 833–844. https://doi.org/10.1016/j.cell.2015.04.011

Fig 7

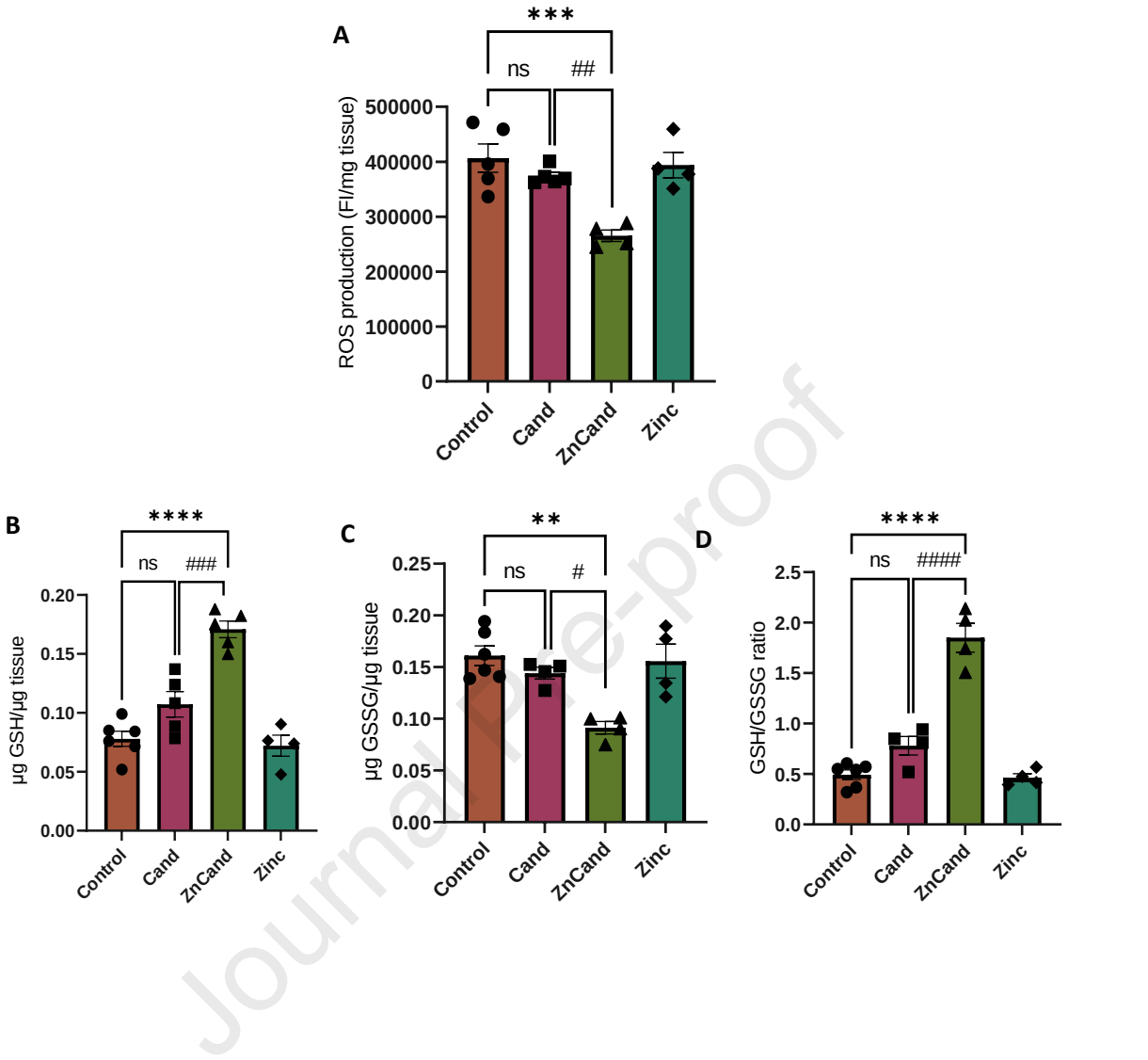

E

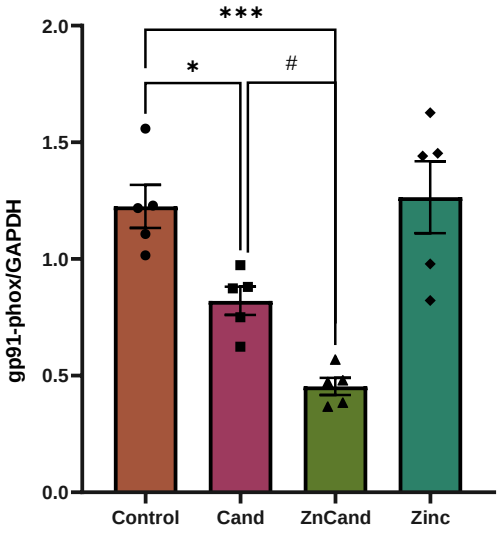

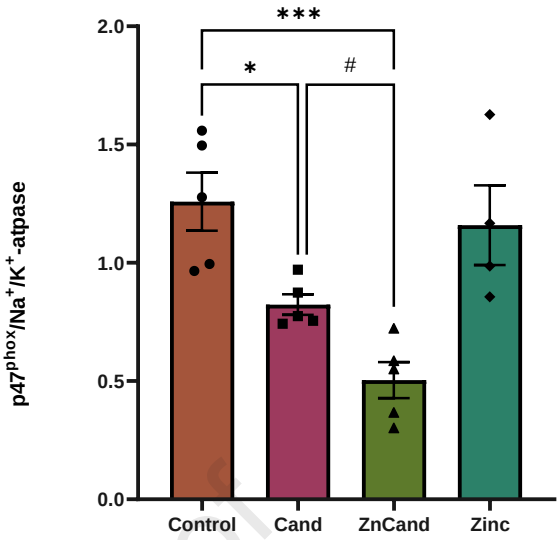

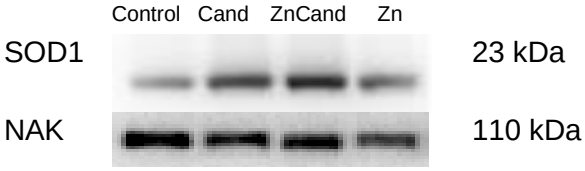

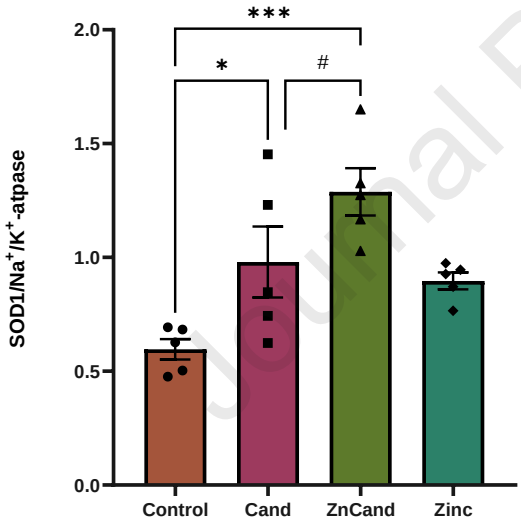

Declaration of interests

☒ The authors declare that they have no known competing financial interests or personal relationships that could have appeared to influence the work reported in this paper.

☐The authors declare the following financial interests/personal relationships which may be considered as potential competing interests: